

# SENSUM

Framework to integrate Space-based and in-situ sENSing for dynamic vUlnerability and recovery Monitoring

FP7-SPACE-2012-1 Collaborative Project **312972**

## Deliverable

<b>Deliverable</b>	<b>Case studies on data-rich and data-poor countries</b>		
<b>D5.3</b>			
<b>Work package</b>	5	<b>Status (F=Final, D=Draft)</b>	F
<b>File name</b>	SENSUM_D5.03_FINAL_V1		
<b>Dissemination Level (PU=Public; RE=Restricted; CO=Confidential)</b>			PU

## Document Control Page

Version	Date	Comments
1	31.08.2014	First draft
2	30.11.2014	Draft for review
3	13.01.2015	Final check (K.F.)
4	04.02.2015	Final version, uploaded to ECAS

Authors	
Name	Institution
Dilkushi de Alwis Pitts	University of Cambridge
Enrica Verrucci	University of Cambridge
Alessandro Vicini	ImageCat Ltd.
Shifeng Wang	University of Cambridge
Emily So	University of Cambridge

<b>Deliverable Leader</b>	<b>Name</b>	Emily So
	<b>Institution</b>	UCAM
<b>Keywords</b>	disaster recovery, methods, protocols, monitoring, remote sensing	

## Table of contents

Document Control Page .....	2
TABLE OF CONTENTS.....	iii
LIST OF FIGURES .....	iv
LIST OF TABLES.....	iv
EXECUTIVE SUMMARY .....	6
1Introduction.....	7
2Summary of findings from previous deliverables and implications for WP5.....	8
3Case Study Application.....	22
3.2 Accessibility Analysis.....	30
3.3 Camp Detection Tool.....	42
3.3.2 Method .....	42
3.4 Open Spaces Assessment .....	50
3.4.3 Results .....	53
4Conclusions and Future Work .....	63
REFERENCES .....	64

## List of figures

Figure 2.1 Table showing the main requests for information from the scenario planning game at early recovery and monitoring and evaluation of post-disaster recovery.....	10
Figure 2.2 Diagram illustrating the two-tier approach taken by SENSUM to use moderate resolution imagery to pinpoint areas of focus and high resolution imagery for asset and change detection of the five recovery indicators. ....	12
Figure 2.3 Accessibility workflow for the monitoring and evaluating the presence of and changes to roads over the recovery period. ....	15
Figure 2.4 Building workflow for monitoring and evaluation of the presence and changes to buildings over the recovery period. ....	18
Figure 2.5 A camp analysis workflow for the evaluation of the number of tents in camps. ....	20
Figure 2.6 Workflow diagram for the monitoring recovery progress by the removal of camps (and change detection). ....	21
Figure 2.7 Final workflow for camps analysis for early recovery, monitoring and evaluation. ....	22
Figure 2.8 Workflow diagram for the assessing operational status of critical facilities by change detection.....	24
Figure 3.1 showsthe initial shift between the raw satellite Quickbird image acquired for the case study of Muzaffarabad, Pakistan, and the Google Satellite background map, used as the reference image. ....	26
Figure 3.2 The yellow line on the left side of the road is a useful reference to understanding how well the shift has been corrected after the co-registration. ....	27
Figure 3.3 Sequence of images showing the improvement of the alignment of the Quickbird - 13 <sup>th</sup> August 2004 - acquired for Muzaffarabad, Pakistan on the Google Satellite reference map, using the yellow road line as the reference.....	28
Figure 3.4Satellite data for Van .....	29
Figure 3.5 Imagery and Data Acquisition dates .....	30
Figure 3.6 Van, Turkey, OpenStreetMap layer overlaid over a high resolution image .....	31
Figure 3.7 Primary and secondary roads for Van are shown in yellow overlaid on a high resolution image. The attribute table in the side show that the data are well populated.....	31
Figure 3.8 Muzaffarabad, Pakistan – Digitized primary (red) and secondary (yellow) roads.....	32
Figure 3.9 Pre-disaster QuickBird image of Kashmir, Pakistan, clipped by the buffered primary roads. ....	36
Figure 3.10Post disaster QuickBird image of Kashmir, Pakistan clipped by the buffered primary roads. This image was taken 14 days after the earthquake.....	37
Figure 3.11 The Normalized roughness difference between pre- and –post-PAN images pertaining to the primary roads. ....	38

Figure 3.12 The Normalized difference in the edges between pre- and post-infrared images pertaining to the primary roads..... 39

Figure 3.13 The Normalized difference in the gradient between pre- and post-PAN images pertaining to the primary roads..... 40

Figure 3.14 a) and b) are the pre- and post-images of the clipped roads. By looking at these images, a visual index of 2 was determined because the roads have not changed much between the two images. C) and d) show a considerable change, hence a value of 9 is used as the visual index. 30 road segments were visually analysed and an appropriate visual index determined ..... 42

Figure 3.15 The visual index for randomly selected road segments are shown in the above figure.... 43

Figure 3.16The Enhanced Change Detection Index is shown for all the roads. This is an indicator of degree of change between the pre- and post-disaster images..... 44

Figure 3.17 Visual Index vs. Enhanced Change Detection Index(ECDI) for all the roads. Visual Index and ECDI show a linear relationship for the roads. .... 45

Figure 3.18 Evolution of a camp site over the time period from the acquisition of the pre-image and the Post3 (recovery) image. The Post 1 image shows the existance of camps while the Post 3 show camps being removed..... 50

Figure 3.19 SENSUM plugin for camp detection. Several combinations of the two variables (max area and Threshold coefficient) have been tested..... 51

Figure 3.20 The camps identified by the described method..... 52

Figure 3.21 The distribution of automatically extracted tents polygons on the input image. .... 53

Figure 3.22 The camp detection function based on image morphology was tested at an open space in Van, Turkey. The camps detected from are shown in purple. .... 54

Figure 3.23 Workflow of the open area detection and detection of camp grounds..... 56

Figure 3.24 Open Spaces for Van Turkey are shown in green and are overlaid on a GeoEye image of a greater extent. .... 58

Figure 3.25 Zoomed in version of a pre-disaster image showing the open spaces..... 59

Figure 3.26 Zoomed in version of a post-disaster image showing camps in the open spaces. .... 60

Figure 3.27 Normalized difference between the pre- and post-images pertaining to the open areas only. The open areas with camps show more texture than those areas with none. .... 61

Figure 3.28 The Normalized difference of the edges with the open spaces. .... 62

Figure 3.29 Normalised difference of the gradient within the open spaces. .... 63

Figure 3.30 The visual index obtained from looking at the pre- and post-images of the open spaces.65

Figure 3.31The Enhanced Change Detection Index obtained for each of the open spaces. .... 66

Figure 4.1 Idealised recovery curve (Lallement, 2013)..... 67

## List of tables

Table 3.1 shows the initial shift between the raw satellite Quickbird image acquired for the case study of Muzaffarabad, Pakistan, and the Google Satellite background map, used as the reference image. ....	26
Table 3.2 Satellite data for Van.....	29
Table 3.3 Imagery and Data Acquisition dates.....	30

## Glossary of Terms

GFZ	German Research Centre for Geosciences, DE
EUCENTRE	European Centre for Training and Research in Earthquake Engineering, IT
DLR	German Aerospace Center, DE
NGI	Norwegian Geotechnical Institute, NO
UCAM	University of Cambridge, UK
CAIAG	Central Asian Institute for Applied Geosciences, KG
IGEES	Institute for Geology and Earthquake Engineering, TJ
ICAT	ImageCat Ltd., UK
EC	European Commission
WP	Workpackage
DoW	Description of Work
GCP(s)	Ground Control Point(s)
QGIS	Quantum GIS

## Executive summary

The aim of Work Package 5 is to assess the needs of decision makers and end-users involved in the process of post-disaster recovery and to provide useful guidance, tools and recommendations for extracting information from the affected area to help with their decisions. This report follows from Deliverables D5.1 “Comparison of outcomes with end user needs” and D5.2 “Semi-automated data extraction” where the team had set out to explore the needs of decision makers and suggested protocols for tools to address their information requirements. This report begins with a summary of findings from the scenario planning game and a review of end user priorities; it will then describe the methods of detecting post disaster recovery evaluation and monitoring attributes to aid decision making.

The proposed methods in the deliverables D2.6 “Supervised/Unsupervised change detection” and D5.2 “Semi-automated data extraction” for use in post-disaster recovery evaluation and monitoring are tested in detail for data-poor and data-rich scenarios. Semi-automated and automated methods of finding the recovery indicators pertaining to early recovery and monitoring are discussed.

Step-by-step guidance for an analyst to follow in order to prepare the images and GIS data layers necessary to execute the semi-automated and automated methods are discussed in section 2. The outputs are presented in detail using case studies in section 3. In order to develop and assess the proposed detection methods, images from two case studies, namely Van in Turkey and Muzaffarabad in Pakistan, both recovering from recent earthquakes, have been used to highlight the differences between data-rich and data-poor countries and hence the constraints on outputs on the proposed methods.

*Keywords:* earthquakes, recovery, evaluation, scenario, protocols.



# 1 Introduction

After a major disaster, time is compressed and there is an urgency to bring relief and to 'get back to normal' – to rebuild livelihoods, clear up the debris, repair the damage and, amongst the more far-sighted, to 'build back better'. This means that decision making happens much faster and under more pressure than normal. Experts come together for a limited time, usually less than two years, and are given extraordinary powers to get things done.

The proposed methods in D2.6 "Supervised/Unsupervised change detection", and D5.2 "Semi-automated data extraction" for use in post-disaster recovery evaluation and monitoring are tested in detail for data poor and data rich scenarios are then presented in detail using case studies in section 3. The process an analyst would need to follow to prepare the images and layers, and step by step guidance on how to execute the methods are included in this section. In order to develop and assess the proposed detection methods, images from two case studies, namely Van in Turkey and Muzaffarabad in Pakistan, both recovering from recent earthquakes, have been used to highlight the differences between data rich and data poor images and hence the constraints of output on the proposed semi-automated and automated methods. It must be emphasised that remote sensing is not the answer, but a means to an answer. Our challenge as academics and practitioners is to devise a way to enable decision makers to make informed decisions in a more efficient way. WP5 aims to provide solutions for different base conditions and scales, in line with end-user capacities and needs.

## 2 Summary of findings from previous deliverables and implications for WP5

The section below is a short summary of the findings from previous SENSUM deliverables and their implications for the identification of standard indicators and workflows for the dynamic mapping of post-disaster recovery for evaluation and monitoring purposes.

### Finding 1 - Users preferences

The scenario game described in Deliverables D4.1 “End-user assessment” and D5.1 has revealed that in the early recovery phase, end-users prefer “quick and dirty” products over detailed maps and databases. Nonetheless, information needs seem to change dramatically with time, with end-users moving their interest to products of greater detail and accuracy in order to support the recovery monitoring and evaluation phase and to gather data for the following vulnerability assessments and planning/mitigation operations (Table 2.1).

Figure 2.1 Table showing the main requests for information from the scenario planning game at early recovery and monitoring and evaluation of post-disaster recovery.

		Early Recovery	Monitoring and Evaluation
A	Accessibility	<ul style="list-style-type: none"> <li>Extraction of damage to road network, which includes primary and secondary roads and bridges</li> <li>Accessibility</li> <li>Proximity analysis</li> <li>Traffic activity analysis</li> </ul>	<ul style="list-style-type: none"> <li>Extraction of recovered primary and secondary roads</li> <li>Extraction of new primary and secondary roads</li> <li>Accessibility</li> <li>Proximity analysis</li> <li>Traffic activity analysis</li> </ul>
B	Buildings	<ul style="list-style-type: none"> <li>Building density of damaged buildings</li> <li>Estimated Population density in damage buildings to inform sheltering and re-housing</li> </ul>	<ul style="list-style-type: none"> <li>Building density at different stages of the recovery/ reconstruction process</li> <li>New estimated population for reconstructed and new building stock</li> </ul>
C	Camp	<ul style="list-style-type: none"> <li>Land-use/open spaces</li> <li>no. of camps</li> <li>no. of tents per camp</li> </ul>	<ul style="list-style-type: none"> <li>New land-use/open spaces</li> </ul>
D	Infrastructures	<ul style="list-style-type: none"> <li>Detailed analysis of utilities and services infrastructure and its operational status ( night-light)</li> </ul>	<ul style="list-style-type: none"> <li>Detailed analysis of utilities and services infrastructure and its operational status ( night-light)</li> </ul>
E	Land Use – Environment	<ul style="list-style-type: none"> <li>Land- use / open spaces</li> </ul>	<ul style="list-style-type: none"> <li>Land- use / open spaces</li> </ul>

As shown in Table 2.1, early recovery indicators are meant to provide information on where change has occurred and how this change is linked to the investments of resources to return to normalcy. The quantification of such indicators is usually repeated during short intervals to track progress. Most typical examples are the traffic activity analysis, which indicates that the road network is accessible and operational, and the camp analysis, which provides information on the number of displaced and on housing/rehousing needs.

Monitoring and Evaluation indicators are instead orientated to assess the long-term effects of the recovery operations and are therefore meant to offer a single, or less frequent, snap-shot of how effective the overall investment of resources has been. Such data are used to build new databases and statistics about the location and the density of the population and on the change in usage of areas previously occupied by temporary camps or vacant. This includes inventories of new roads, new buildings, and a review of the operational status of key infrastructure.

**Implication 1:** SENSUM products need to satisfy diverse information needs. However, both during the early recovery and longer-term monitoring and evaluation phases, the scale of the objects under investigation (e.g., building, camps, and critical infrastructure) limits the application of moderate resolution data. Nonetheless, as one of the purposes of the SENSUM project is to fully exploit the benefit of free-of-charge data sources, an over-arching temporal analysis method to identify areas of change has been developed. Such method, which uses Landsat data as input, is designed to provide preliminary information of which areas are to be the focus of more detailed analysis, and can therefore be used to produce rapid focus maps (see deliverable D3.3 “Focus map implementation”) during the early recovery stages.

The scenario game revealed how the needs of the end-users change dramatically over-time. During emergency response and early-recovery, end-users are interested in products that can help them assess the situation rapidly. The need for more accurate information emerges much later, during the monitoring and evaluation phase of recovery. It was also clear from the game that whilst in the very beginning of the recovery process the users are more interested in understanding where change has occurred, the detailed level of information required for monitoring and evaluating recovery limits the applicability of remote sensing products derived from moderate resolution imagery. Therefore, in order to address the time-dependent needs of the users, we have developed two different approaches, still focusing on the five physical recovery indicators.

The first approach exploits the much larger extent of moderate resolution images to detect areas of changes. As Landsat data can be acquired at no cost from the fairly rich USGS archive, this method is based on the analysis of multi-temporal stacks of images. The second approach uses high resolution data to understand how and why change has occurred. This is shown in Figure 2.1.

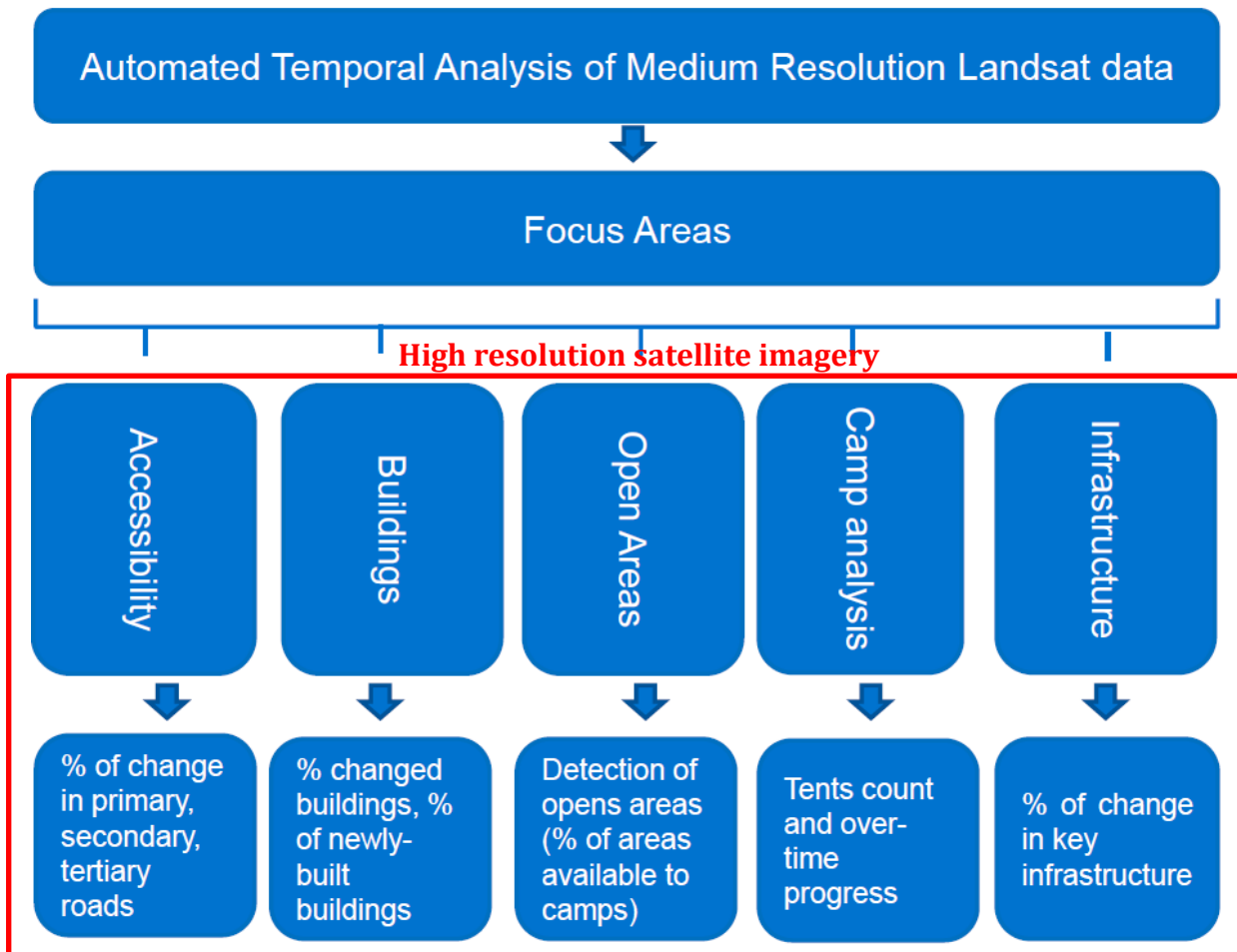


Figure 2.2 Diagram illustrating the two-tier approach taken by SENSUM to use moderate resolution imagery to pinpoint areas of focus and high resolution imagery for asset and change detection of the five recovery indicators.

**Finding 2 - Workflows for post-disaster recovery evaluation and monitoring**

In Deliverable D5.2, five different workflows were suggested, one for each of the physical recovery indicators identified in Table 2.1. These are accessibility, buildings, camps, infrastructure, and land-use/environment.

Such workflows were mostly based on theoretical research and on previous studies (e.g., the ReBuildDD project) and suggested a preliminary idea of how specific indicators could be extracted. This section improves on the conclusions of the previous deliverable by offering more detailed workflows which incorporate the progress of the developed SENSUM plug-ins from WP2.

## **Implication 2 - Variation suggested for each workflow**

### **A) Accessibility**

For both early and long-term recovery monitoring and evaluation, accessibility analyses over time would provide information on the operational status of the road network in the affected area.

For early recovery, end users may wish to assess road damage to evaluate difficulties in aid supply and transport logistics, as well as for locating potentially isolated communities. For monitoring and evaluation, data are needed to estimate what percentage of roads was repaired and rebuilt and what roads have been newly-built to alleviate the limits of the pre-disaster road network as well as for connecting to new urban settlements.

As mentioned in deliverable D5.2, several remote sensing techniques can be applied to the isolation of the road surfaces from the rest of the classes of the image. Nonetheless, both automated and semi-automated methods, either pixel- or object-based, show significant limitations. From a spectral point of view, urban roads are often very similar to roof tops and other impervious surfaces. Similarly, rural roads may be difficult to identify due to the lack of contrast with the surrounding soil and also due to their limited width (e.g., rural paths and tracks). From an object-based stand point, roads can be difficult to extract as continuous objects, especially when high-rise buildings or vegetation overshadow them. Furthermore, as results greatly vary with each scene, such methods may not be suitable for multi-temporal studies and, being quite complex, they would still require a certain degree of proficiency of the analyst, who will ultimately need to visually verify the outputs.

Although analysts should always verify the applicability of such methods to each case's specific condition, it is not easy to suggest a single method that would result in sufficiently accurate information for each case study whilst also complying to the need for rapid information in the early recovery phase.

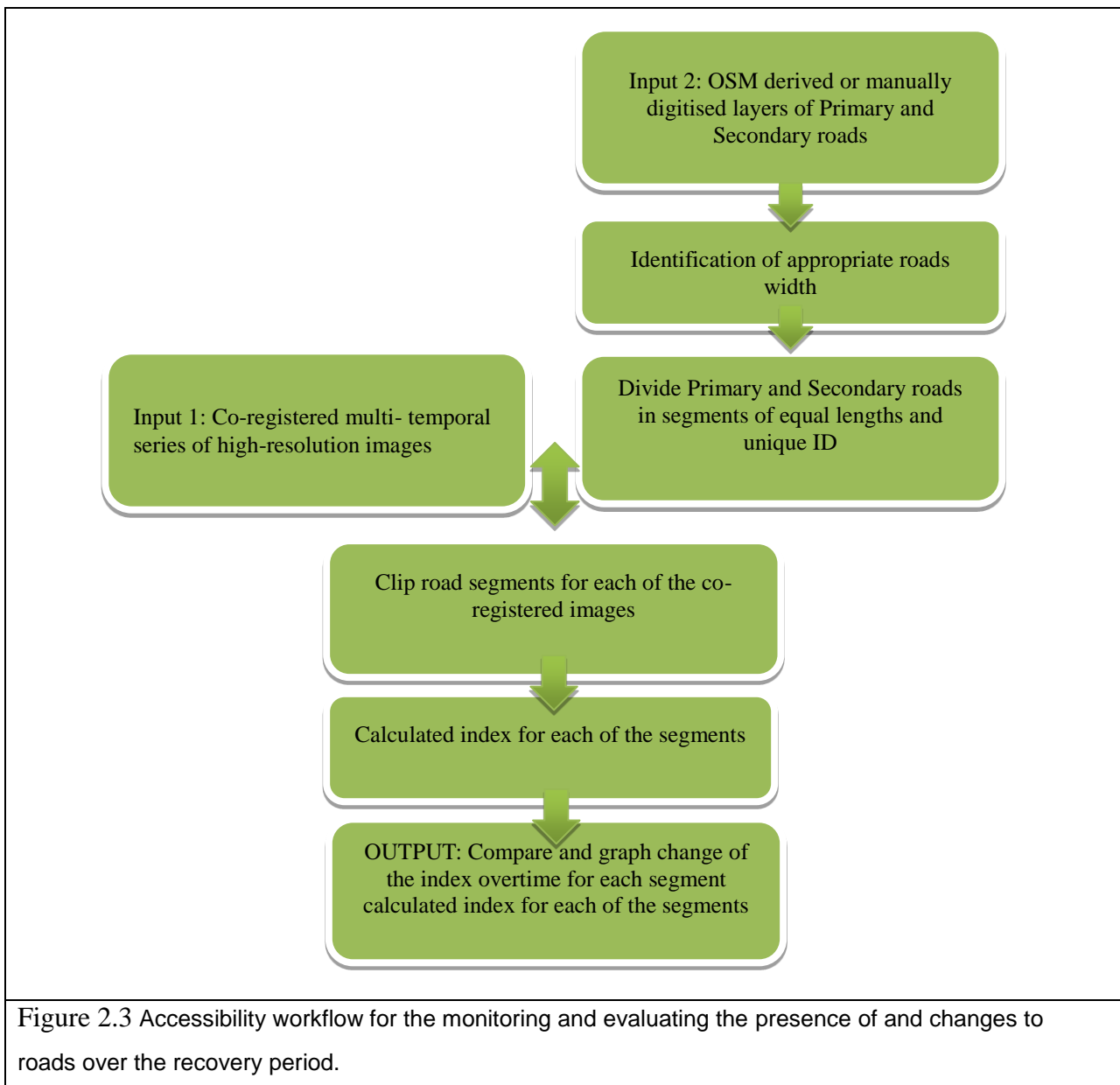
That said, two important considerations have to be taken into account when discussing accessibility. Firstly, the scenario game has confirmed that end-users are usually focused on knowing the operational state of only primary and secondary roads. Secondly, it is important to state that road layers do not necessarily need to be extracted from satellite imagery with automatic or semi-automatic extraction. Nowadays other resources, like OpenStreetMap (OSM), can supply road layers in vector format. OpenStreetMap layers are usually well detailed for developed countries and are becoming more and more diffused in developing countries. Also, should OpenStreetMap data not be available, the user may still consider manually digitising the roads. Such a procedure should not be too onerous if limited only to the primary and secondary road networks and can be easily performed by users of all levels of expertise.

Once the vector road layer is available, the next step is to understand how wide the primary and secondary roads are. The user can check this by installing the Open Layers plugin available in the plugin library of QGIS and use the ruler tool to measure the width manually. It is good practice to measure the width in several points of the road network and calculate an average width. The user can then apply a buffer to each one of the raster images in the temporal series. Each high resolution image can then be clipped and analysed with a change detection algorithm built ad-hoc for accessibility analysis.

Hence, the modified workflow is as in Figure 2.2.

All phases of this workflow can be performed in an automatic or semi-automatic way using either functions that are already available in QGIS or functions available through the SENSUM plug-ins. The first input of the workflow is a multi-temporal series of high resolution images. The images need to be co-registered. If the first (usually pre-disaster image) is not aligned to the reference map, the analyst will need to correct the alignment using the Georeferencer, a tool already available in QGIS and located under the Raster tab on the main menu.

The first image of the temporal series is co-registered on the map by displaying Google maps as a background layer in QGIS. This process is then repeated for the rest of the images, this time displaying the newly co-registered first image as the reference layer and in the Georeferencer window each of the remaining images in the temporal series. A detailed description of the co-registration process for the case studies of Van in Turkey and Muzaffarabad in Pakistan can be found in Section 3.1



The second input to the workflow is the street layer. Again, QGIS has a very useful resource to download road layers in a vector format. The analyst can download the road layer directly from the OpenStreetMap archive by clicking on the Vector tab on the main command menu and moving to OpenStreetMap -> Download data. The analyst is then prompted to decide the extent of the layer to be downloaded and to save it as an output file.

When dealing with accessibility studies, having an idea of the hierarchy of the road network can be

useful to distinguish primary and secondary roads from the others. Some information to this regard can be found in the attribute table of the OSM downloaded vector file. However, it is important to note that the degree of completeness, as well as the quality, of information contained in the attribute table may differ greatly from place to place. Therefore, it may be appropriate for the analyst to check if the OSM layer is already sufficient or if manual amendments and additions are required.

Irrespective of the vector road layer being downloaded from OSM or created by the analyst manually, the vertices of the road layer can always be shifted at any time to create a better alignment with the images or maps.

Once the best alignment has been reached, the road layer can be buffered. The buffer width can be estimated by measuring on a Google map the average width for the specific level of roads. Before proceeding with the buffer, it is appropriate to re-project both co-registered images and road layer to an UTM projection, so as to keep the reference units of the maps in meters. To obtain segments of roads in the same lengths, the geometry of the road layer is first merged as each road layer was constituted by one single road and then split with the Split by length QGIS algorithm. Then the analysis can be applied to the buffer to each of the segments. This process is done automatically with QGIS.

Each of the buffers can then be used as a clip mask for the individual co-registered raster layers in the temporal stack.

Using the change detection HR algorithm in the SENSUM plug-in, it is possible to provide an estimate of the amount of change over-time for each of the clipped images and therefore provide a rapid mapping of how the whole road layer has been affected by change within the time period covered by the temporal stack of high resolution images.

A word of caution is required here. A number of factors can produce changes in an image. Restricting the analysis to small segments of the image (the clips) can help focus on more local abrupt changes rather than generalised changes in the image (e.g., illumination). Nonetheless, the resulting maps of change need to be evaluated by the analyst to detect effects in the image that can produce changes that are not disaster or recovery related. Visual interpretation is therefore required for the final validation of results. The case study description in Section 3 will further detail



this process and limitations to the described method using examples and comparisons.

## B) Buildings

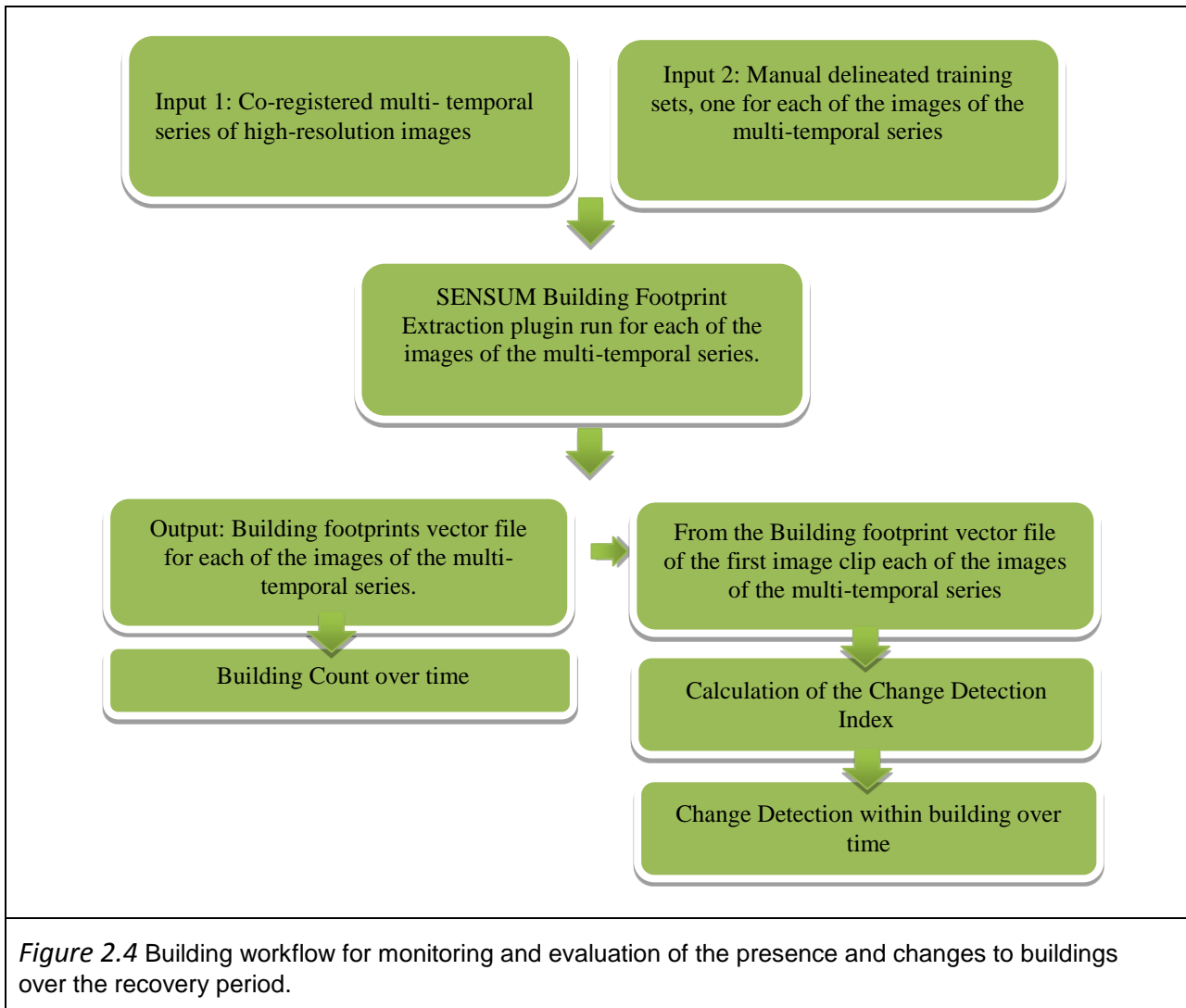
Building analysis is another crucial aspect of recovery monitoring and evaluation as the number of buildings is a proxy for other information such as population density.

The number of buildings is calculated by using the SENSUM Building Footprint Extraction plugin. The plugin requires as input a VHR multi-spectral satellite image and a training set. The analyst points the algorithm to the input image file and to the correspondent training set. Although the aim of the algorithm is to extract only the building footprints, it is good practice to include in the training set examples of each of the visible classes in the image, which include each building type and roof colour, open areas, roads, bare lands, and vegetation. A good training set usually consists of more than one example for each of the identified classes, as this allows the analyst to understand ranges of spectral variation within each class, thus allowing for a neater differentiation of the classes.

The algorithm runs in sequence an optional smooth filter and a supervised classification. Based on the results of these preliminary steps, it proceeds with the extraction of the objects associated with the classes identified by the analyst as roof types. This process is followed by a morphological and an area filter. The Building footprint output is a vector file.

By repeating this operation for all the images in a multi-temporal series, it is possible to evaluate how the number of buildings has changed over-time. It is important to know that, since the results are dependent on the output of the supervised classification, the creation of the training set is a crucial aspect of this algorithm. The choice of a good training set can help to significantly reduce the misclassification errors.

Hence, the modified workflow is as in Figure 2.3. The Building Extraction Footprint vector file for pre-disaster image is used as the reference image to assess the change of the number of buildings over time. The contours of the buildings identified in the pre-disaster image are also used to clip all the images of the temporal series so that changes in the spectral appearance of each building can be assessed over-time. Again, as in all the applications of the change detection index, not all the changes identified are linked to recovery. Visual interpretation is necessary to validate the results.



### C) Camps

Camp analysis is a crucial tool that can be used by end-users to assess post-disaster recovery progress. In the early recovery phase, the number of tents in a camp can be used as a proxy to assess displaced population and thus plan provisions for temporary housing. In the monitoring and evaluation phase, end-users are interested in verifying that all the population is being progressively rehoused and that the areas previously occupied by the camps are vacated or re-allocated to a different usage.

Tent-related information that is extracted from satellite imagery is often carried out by visual interpretation (Giada et al., 2003; Bjorgo, 2000b). The ReBuiDD project (Brown et al., 2013) investigated how camp analysis can be performed using both classification techniques and manual counting. The SENSUM team has built on the findings of this research and has proposed a novel

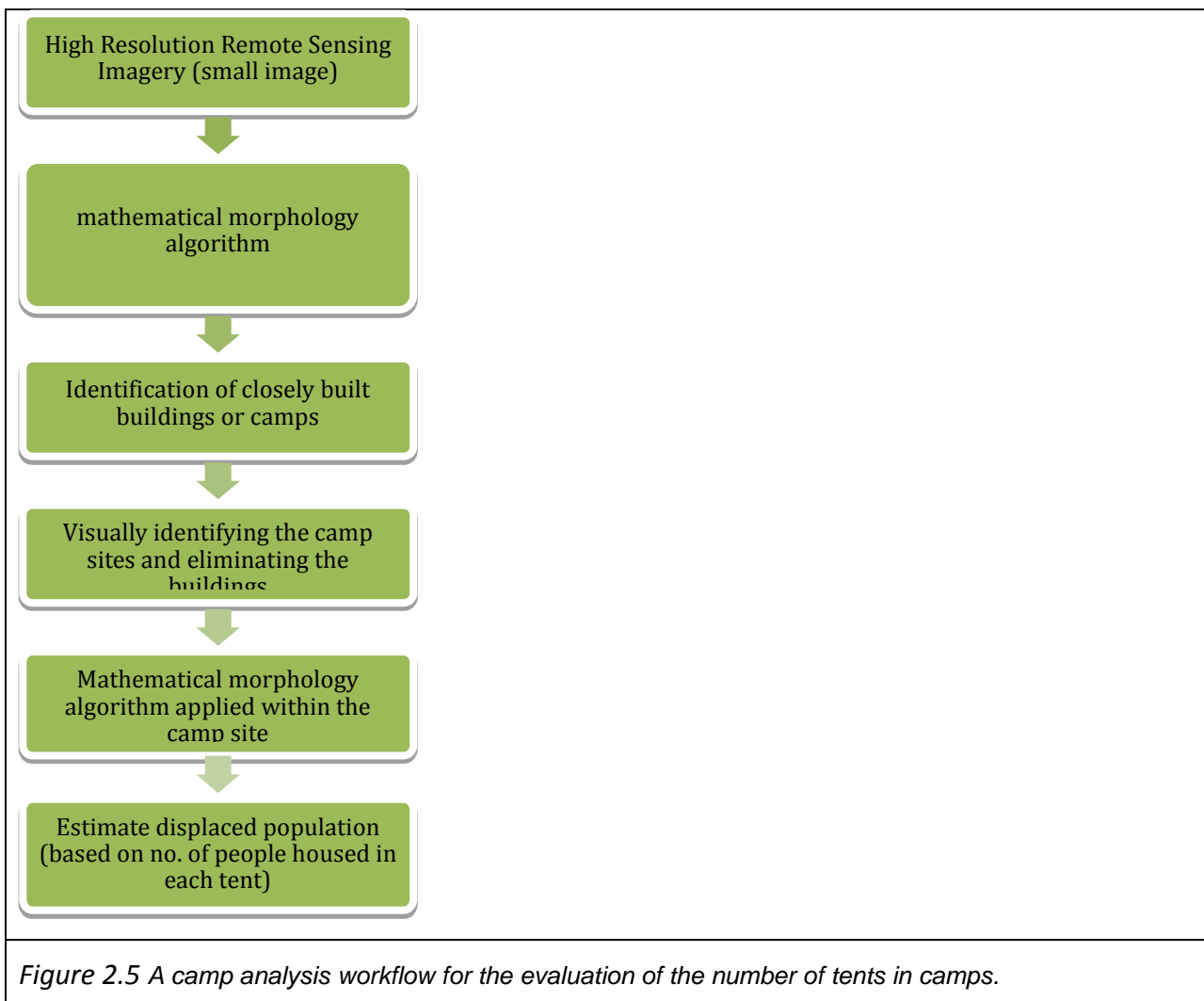
approach to automatically count tents, which involves the use of mathematical morphology. Visual interpretation of high resolution imagery is accurate, but very time consuming and labour intensive, making it difficult to apply to relief operations following a disaster. Semi-automatic and automatic methods have been suggested, but there has been little research. Giada et al. (2003) used four methods to detect the refugee tents at the Lukole refugee camp in Tanzania: pixel-based supervised classification, unsupervised classification, mathematical morphology and the object-based segmentation and classification. Comparing the performance of these four methods, they found that mathematical morphology and the object-based segmentation and classification performed better than pixel-based supervised classification and unsupervised classification. The mathematical morphology method is based on the assumption that most tents are of standard dimensions, therefore each single tent can be identified with a high degree of accuracy if the algorithm is trained to recognise shapes of specific dimensions. The method includes four steps: morphological opening, opening by reconstruction, top-hat by reconstruction, and morphological threshold. This method is especially useful for objects characterised by the clear shape, size and contrast. It uses the morphological erosion and morphological dilation to identify targeted objects such as tents.

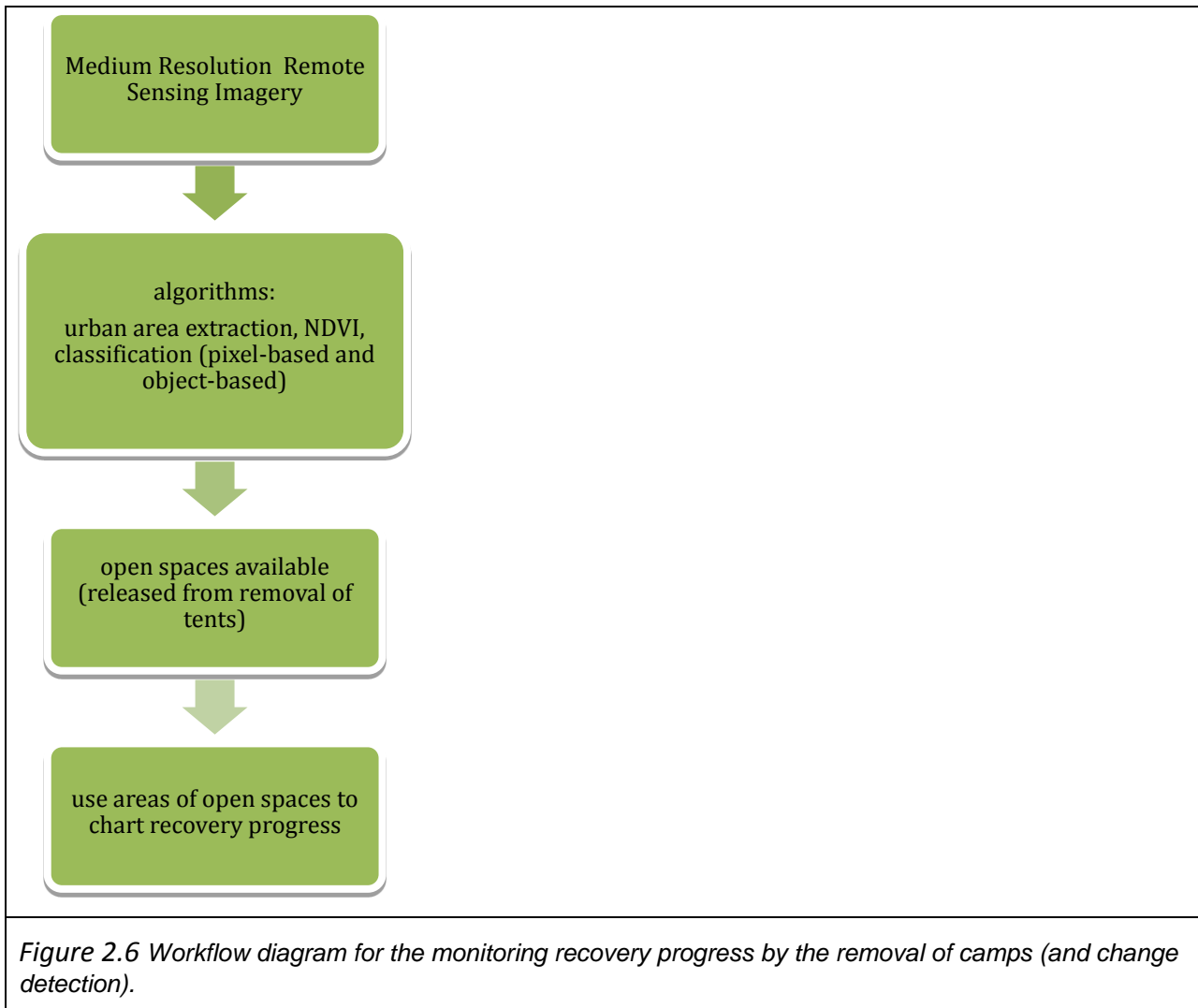
Before one begins to investigate the possibility of automated methods for tent detection, one must first set the rules to filter out tents from other aspects of urban built up areas. Camp villages are composed of tents which are mainly provided by relief organisations such as Red Cross and thus have standardised designs and regulations. Tents have a regular structure and a distinctly different spectral and texture from urban buildings. The characteristics we can use to identify these automatically with a computer are spectral, spatial (area and shape), and texture (compactness and smoothness).

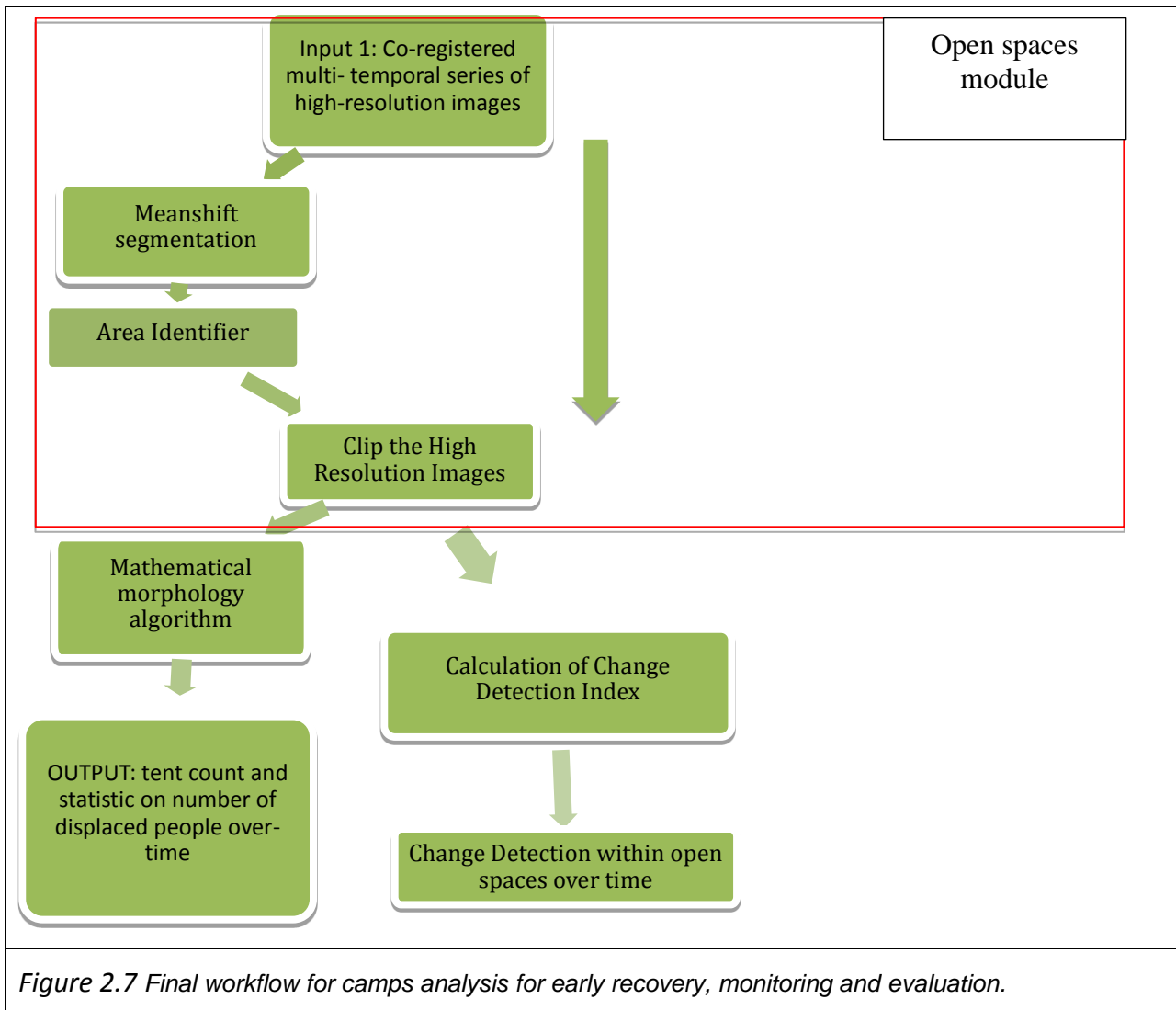
Several tests have been run to understand how to calibrate each variable (e.g., tent dimensions, thresholds coefficients described in section 3.3) and obtain the best results in terms of tents count. Although the dimensions of the tents are often significantly smaller than buildings, misclassification errors are possible. To avoid buildings being mistakenly counted as tents and to increase the accuracy of the method, the workflow has been modified to include a step in which the open spaces which can be used to place camps are identified and clipped before the clips are analysed with the mathematical morphology algorithm. A meanshift segmentation algorithm is used to isolate open spaces (Figure 2.5). Not all the open spaces are big enough to allocate camps. As the segmentation returns as output a vector file, the size of each segment can be calculated and the

user can then visual interpret which of the larger segments are actually open spaces. The contours of such segments can then be used to clip the multi-temporal series of images, on which the morphological filter can be applied.

The main advantage of the mathematical morphology method is that it can be run very quickly. Actually, the running time was shown to be directly proportional to the size of the image. So even for large remote sensing imagery, it will only take a couple of minutes to generate an output map. The final output of the method is a layer of tents, so it is possible to account for the number of tents, and the overall area occupied by tents with the aid of other GIS software. Another specific requirement for this method is the resolution of remote sensing imagery in which each tent has to occupy at least six pixels.







#### D) Infrastructure

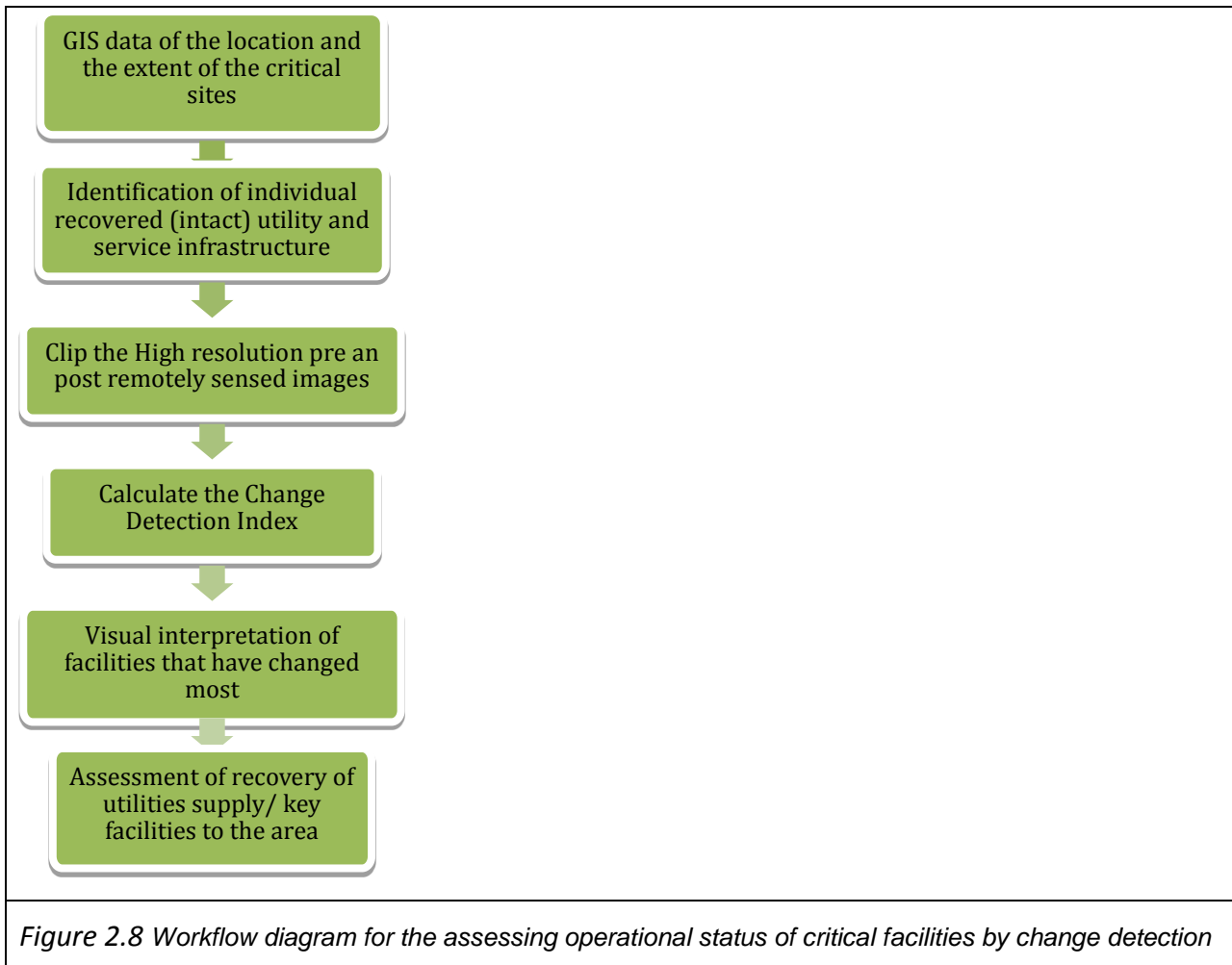
Obtaining information with regards to the operational status of critical facilities and lifelines networks is certainly a crucial requirement for end-users. Nonetheless, as already mentioned in Deliverable D5.2, remote sensing technologies offer limited means to gauge detailed information about such infrastructure and most often the operational status of such facilities can only be directly verified with in-situ surveys. Bearing this in mind, this workflow has been a low priority for the SENSUM project.

With the exception of the road networks, service lifelines (e.g., electricity, oil and gas, water, waste waters) are usually very hard to detect visually as the vast majority of such infrastructure is located below ground and the above ground features, such as electrical substations, do not present

distinctive characteristics which could facilitate their localization in an urban environment. It is also important to note that such services are managed either directly by central governments or by private companies which have their own systems to understand which part of the network is still operational. For such reasons, the infrastructure workflow has not been designed to investigate the operational status of service lifelines.

As for other critical infrastructure - such as hospitals, police, and fire stations - nightlights can be used to provide a preliminary indication of which facilities are operational. This type of investigation, however, assumes that nightlights data are available and that the end-user knows the exact location of such facilities. Furthermore, such analysis may not be sufficient to understand which sections of the structure have suffered unrepairable damage and need to be demolished. Provided that the analyst knows how such critical facilities are arranged, again temporal analysis and change detection can be valuable tools. To this regard, several online resources (e.g., Google Earth, Bing Maps) can help a non-local user locate critical structures within the facility.

Once those are identified, the analyst can proceed with the identification and count of damaged, demolished, and rebuilt facilities over time. The two preliminary workflows are therefore modified as in Figure 2.7.



As this method uses visual interpretation for the detection of damage, the case studies do not list an example of this workflow.



### 3 Case Study Application

This section provides the case studies analysed by the SENSUM team to evaluate which remote sensing technologies and SENSUM tools can be used to map and understand change. Automated medium resolution temporal analysis have been performed for the case studies of Cologne in Germany to detect focus areas of urban change. Detailed descriptions of the methodology are presented in Deliverable D2.6 “Supervised/unsupervised change detection” (see section 4). Table 3.1 lists the case studies for the semi-automated change detection analysis on high resolution imagery, which is the specific focus of this deliverable.


#### Data Acquisition and Pre-processing

The case studies application has required some preliminary steps aimed at acquiring ancillary data (i.e., road layers) and pre-processing the satellite data. For the satellite data, the pre-processing consists of pansharpening the multi-spectral images and the manual co-registration of the images to the Google background map, which is available in the Open layer plugin of QGIS, and some downloaded GIS data. For the road layer the process of acquisition has been performed by either downloading the data from the OpenStreetMap layer or by manually digitising the road layers in QGIS, using as the reference map the Google Hybrid background, also available in Open layer plugin of QGIS.

#### Satellite data

All the satellite data have been pansharpened and co-registered to the reference map to ensure the best alignment with other data sources in vector format, such as road layers. The pansharpening has been performed automatically using the SENSUM Plugin Pansharpening tool. Of each multi-temporal series of satellite images per case study, the pre-disaster image has been co-registered to the reference map whilst the others have been co-registered to the pre-disaster image after it was co-registered and re-projected in the WGS 84 - UTM reference system.

For the co-registration of the pre-disaster image, Google satellite background maps have been displayed in the standard visualization pane of QGIS. The image to co-register was instead displayed in the QGIS Georeferencer which opens a parallel window to the standard visualization panel. Once both reference map and raw image are respectively loaded in the QGIS visualization

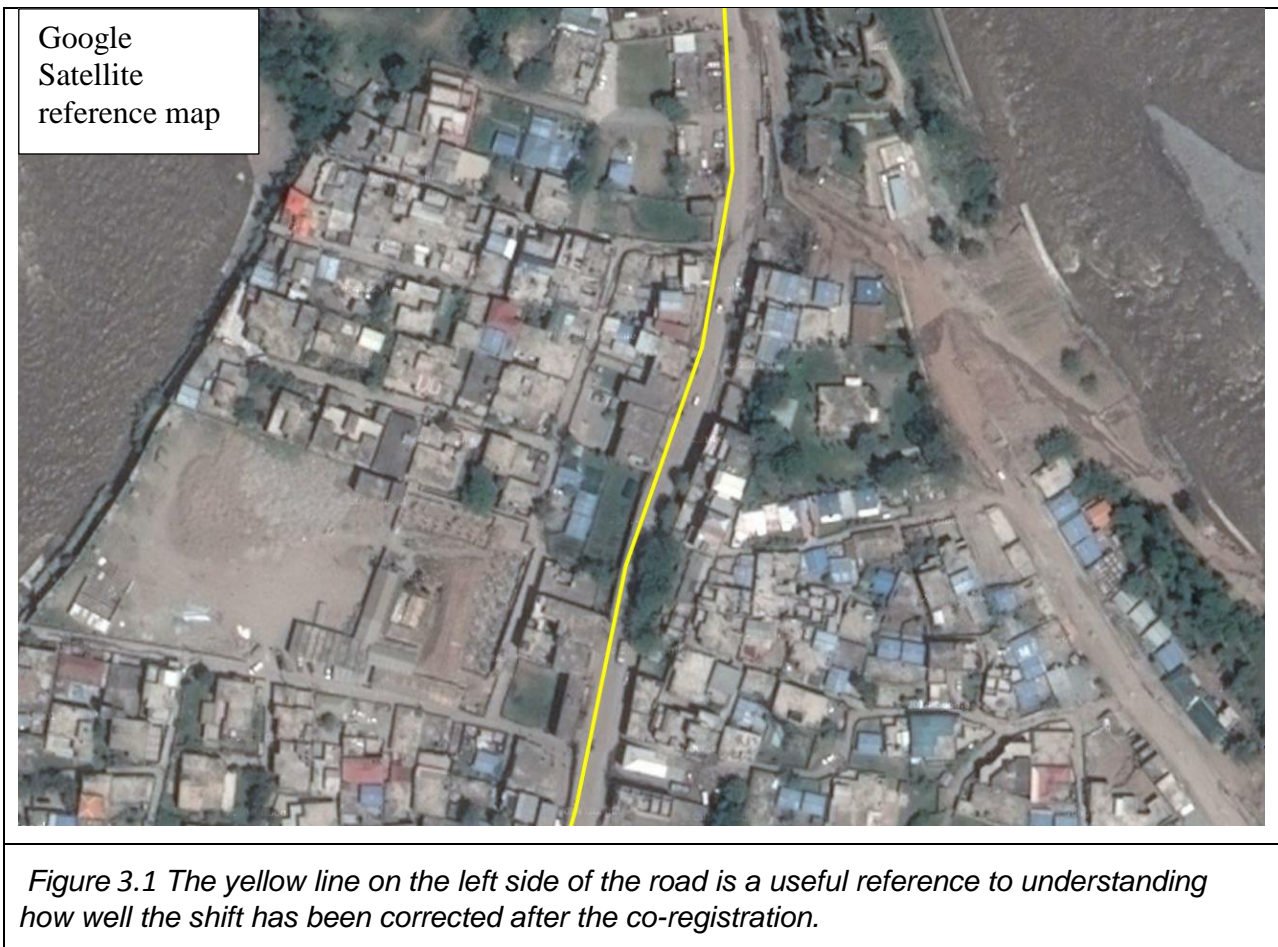
panel and the Georeferencer window, the user can use the “Add point”  icon to progressively detect a sufficient number of reference points on the image and on the map, based on which the algorithm can calculate the adjustments needed to realign the image to the reference map.

The number of points required to perform this operation varies according to the size of the image and to the transformation chosen. For the case studies, the co-registration has been attained using a second degree transformation with a nearest-neighbourhood re-sampling scheme.

The analysts should always try to distribute points uniformly on the image, starting with the corners and moving to the centre. Before running the transformation, it is possible to check how much the shift is between the position given by the analyst to a point and what the correct position for that point should be according to the software. It is appropriate to keep the error associated with the location of each point as close to zero as possible to attain sub-pixel precision in the final co-registration. Figure 3.1 shows the table of the residual, which are purposely kept well below a half-pixel precision.

on/off	id	srcX	srcY	dstX	dstY	dX[pixels]	dY[pixels]	residual[pixels]
<input checked="" type="checkbox"/>	6	353940.87	4270209.37	353947.61	4270254.75	-0.16	0.22	0.28
<input checked="" type="checkbox"/>	4	354111.27	4270183.54	354118.19	4270228.62	0.18	-0.12	0.21
<input checked="" type="checkbox"/>	7	349964.39	4269929.68	349973.34	4269988.00	-0.21	-0.02	0.21
<input checked="" type="checkbox"/>	8	349929.00	4269944.46	349938.13	4270002.77	0.20	0.02	0.20
<input checked="" type="checkbox"/>	5	354004.88	4270155.19	354011.74	4270200.71	-0.09	-0.05	0.10
<input checked="" type="checkbox"/>	1	353276.47	4271413.86	353280.68	4271455.94	0.07	-0.05	0.09
<input checked="" type="checkbox"/>	0	353051.14	4264588.99	353063.89	4264650.83	0.02	-0.01	0.02
<input checked="" type="checkbox"/>	2	363419.59	4266756.33	363426.44	4266761.14	0.00	0.00	0.00
<input checked="" type="checkbox"/>	3	362729.59	4265239.01	362734.76	4265246.82	-0.00	-0.00	0.00

Table 3.1 shows the initial shift between the raw satellite Quickbird image acquired for the case study of Muzzaffarabad, Pakistan, and the Google Satellite background map, used as the reference image.



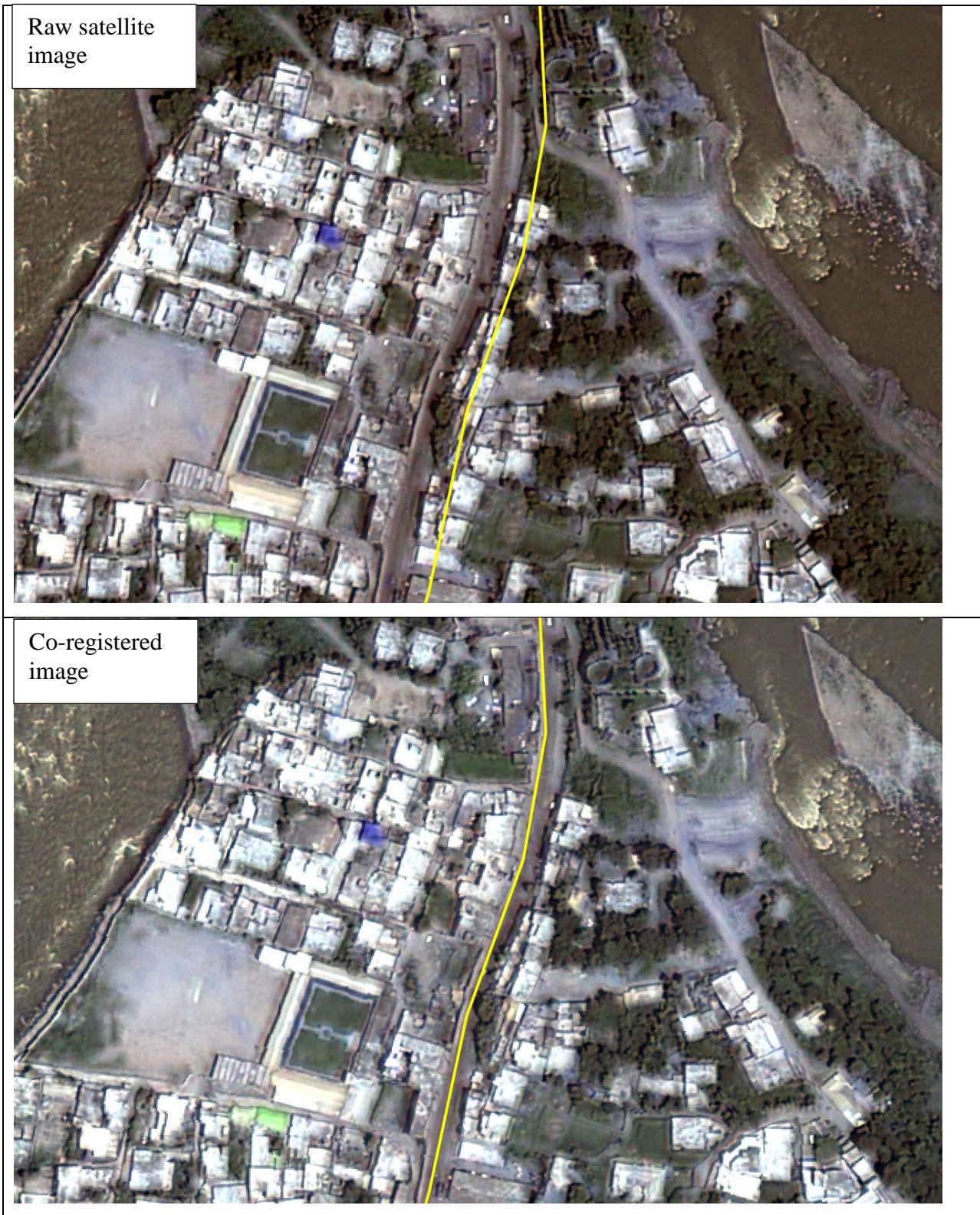


Figure 3.2 Sequence of images showing the improvement of the alignment of the Quickbird - 13<sup>th</sup> August 2004 - acquired for Muzaffargarh, Pakistan on the Google Satellite reference map, using the yellow road line as the reference.

For the case study of Van, 4 satellite images were acquired from 2011 to 2013. The reference event is the Van earthquake, a destructive 7.1 Mw earthquake that struck eastern Turkey near the city of Van on Sunday, 23 October 2011 at 13:41 local time. Based on the reports of the Disasters and Emergency Situations Directorate of Turkey AFAD, the earthquake killed 604 people, and injured 4,152, causing damage to at least 11,232 buildings within the affected region. Of those building, 6,017 were found to be uninhabitable (Wikipedia, 2014).

*Table 3.2 Satellite data for Van*

Imagery	Acquisition Date	Extent	Notes
Pre- disaster	WV02 - 06th May 2011 - 5 months before earthquake	Full scene	
Post 1	12th Jan 2012 - 2.5 months after the earthquake	Half scene - northern portion	
Post 2	22nd Feb 2012 - 3 months after the earthquake	Half- scene southern portion	Snow cover
Post 3	WV02 - 05th June 2013 - 1 year and 7 months after the earthquake	Full scene	

For the case study of Muzaffarabad, Pakistan, three satellite images were acquired from 2004 to 2006. The reference event is the Kashmir earthquake, a destructive 7.6 Mw earthquake that struck the region, near the city of Muzaffarabad, on 8 October 2005 at 08:52 local time. According to the government of Pakistan, the official death toll was 75,000. Of these, around 75% are estimated to have occurred in Muzaffarabad, the state capital of Kashmir (Wikipedia, 2014).

During the co-registration process, the images were clipped to a smaller area covering the central part of Muzaffarabad to exclude the highly mountainous areas on each side of the town. These areas introduced a very high degree of distortion in the original images, affecting the accuracy of the co-registration.

*Table 3.3 Imagery and Data Acquisition dates*

Imagery	Acquisition Date	Extent
Pre- disaster	QuickBird - 13 <sup>th</sup> August 2004 – 14 months before the earthquake	Full scene
Post 1	QuickBird - 22 <sup>nd</sup> October 2005 – 2 weeks after the earthquake	Full scene
Post 2	QuickBird – 13 <sup>th</sup> June 2006 – 8 months after the earthquake	Full scene

The pansharpened and co-registered images have been used as input in the five workflows presented in Section 2. In particular, the pansharpened and co-registered images have been used for the Accessibility, Buildings, Camps, and Open spaces clips. The co-registered panchromatic images have been used in the meanshift segmentation to obtain the contours of the open spaces based on which the multi-spectral images have been cut for the change detection index.

### Preparation of Road layers

The road layers used for the case study are OpenStreetMap vector layers downloaded directly from the Vector tab on QGIS (Vector> OpenStreetMap>Download data) all acquired for the extent of the largest satellite image for each of the case studies. The completeness and level of accuracy of the OpenStreetMap layer varies greatly from country to country. Figure 3.3 shows, for instance, the different levels of completeness of the OSM layer for the case studies of Van, Turkey and Muzaffarabad, Pakistan. For Van, the road layer is well-detailed and the attribute table allows the identification of roads of different hierarchy. For Pakistan however, the road layer is neither complete nor spatially accurate. Therefore, the attribute table is not well populated (Figure 3.3).

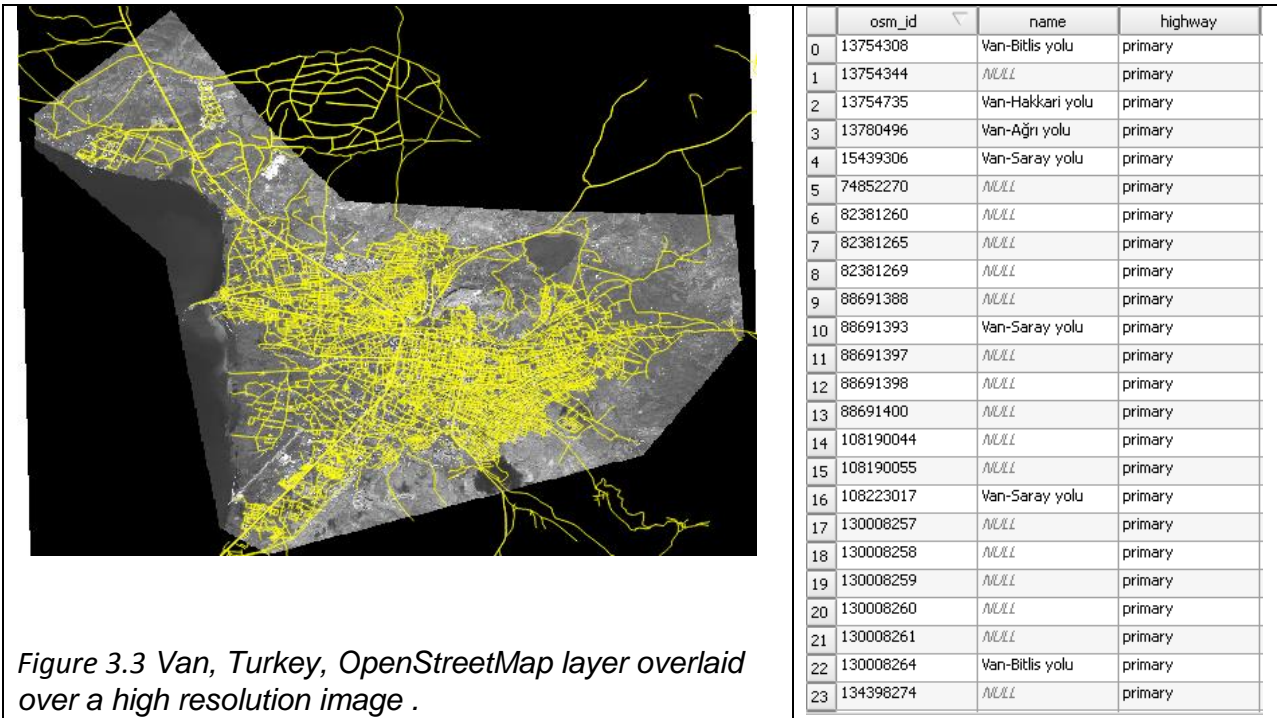


Figure 3.3 Van, Turkey, OpenStreetMap layer overlaid over a high resolution image .



Figure 3.4 Primary and secondary roads for Van are shown in yellow overlaid on a high resolution image. The attribute table in the side show that the data are well populated.

Where for the case of Van, the OSM can be used for the accessibility analysis directly with some

minor adjustment, in the case of Muzaffarabad. it was decided to proceed to manually digitise the street layer for the primary and secondary roads. This can again be done directly with QGIS by simply creating a new shapefile and adding features to it by using the Editor toolbar. The resulting layer for Muzaffarabad is showed in Figure 3.5.

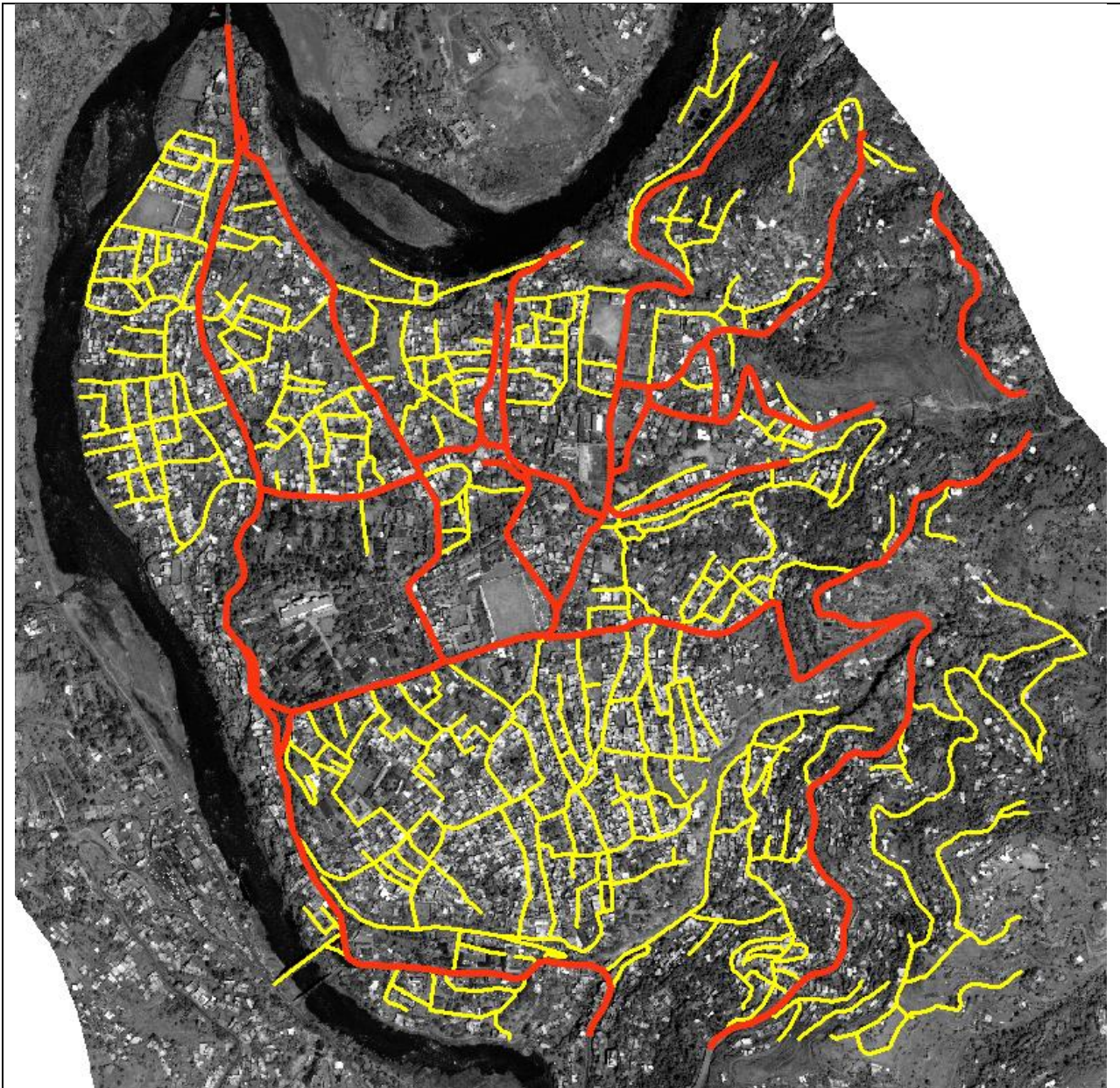



Figure 3.5 Muzaffarabad, Pakistan – Digitized primary (red) and secondary (yellow) roads.

COMMENT ON TIME AND ACCURACY.



Before using the road layer in the accessibility workflow to evaluate the percentages and lengths of the affected roads and the progress of these roads becoming operational, it is important to check that the road layers have the best possible alignment with the roads in the image. When the road layer is systematically shifted, the analyst can improve the quality of the whole layer by correcting

the shift by using the editing function represented by the QGIS icon . If just portions of the road layer are shifted, the analyst can proceed to move the single vertices of the layer using the

editing function represented by the QGIS icon .

### 3.2 Accessibility Analysis

The need to rapidly assess changes on the ground transportation network is the basis of the method created for Accessibility Analysis. The method is based on the hypothesis that in normal conditions, although contour effects may be frequent, the spectral signature of the same portion of road does not change significantly over-time. This means that in conditions of abrupt change, such changes can be rapidly detected and mapped. Conditions of abrupt change can be associated with post-disaster scenarios (e.g., debris on the roads causing road blockages) and also used to monitor recovery/clean-up operations.

The method, illustrated in the workflow in Figure 2.1, requires for each of the satellite images acquired for each specific case study to be co-registered to obtain the best possible alignment to the map and with the images themselves. Both panchromatic and pan-sharpened images have been co-registered for this purpose. The pan-sharpening has been performed using the SENSUM plug-in.

The road vector layer is also required to define the hierarchy and geometry of the network and to identify segments of equal maximum length, each recognised by a unique identifier.

#### Data-critical case study

For the case study of Van, the initial road layer downloaded via OSM was divided into nine layers based on the hierarchy found in the attribute table: Primary, Secondary, Tertiary, Residential, Road, Path, Living Street, Track, and Unclassified. Each of the road layers has been checked to see if

any of the layers intersected the Primary and Secondary road layers, producing discontinuity in the geometry. It was found that the layers were mutually exclusive from a geometry stand point, with no duplication or missing segments in the primary and secondary road layers. So no segments needed to be deleted or manually digitised to complete the geometry.

Looking at the attribute table of both primary and secondary road layers, it was also clear that for the geometry of the polyline, a large number of segments had limited lengths, even when positioned on a straight road. A large number of road segments were generated for analyses after clipping, dependent on the technique with which the OSM users had digitised the track. However, with no apparent benefit to this method, it was decided to simplify the geometry of the road layers by merging small segments as much as possible. This operation was done using the Dissolve algorithm in the Vector> Geo-processing tools of QGIS. Once the geometry was fully dissolved, both Primary and Secondary road layers were split by length using the ***split.by. length*** GRASS command embedded in QGIS. The chosen length was 100 metres, hence the algorithm produced only segments with a maximum length of 100 metres. Due to the geometry of the road layer (e.g., presence of curves) not all the road segments had equal length after this simplification. Nonetheless, as the change index calculates change relative to the length of the segment and given that such a length stays the same across the time series of images, the geometry of the network does not interfere with the relative assessment of change for each given segment of both primary and secondary roads.

The buffer width for each of the road layer was chosen by taking multiple measurements of the road width directly on the pre-image using the measure line available in QGIS. It was decided to apply a 6 m buffer for the primary roads and a 4 metre buffer to the secondary roads.

Each of the segments was then clipped for the complete time series, thus creating the multi-temporal set of raster road segments which are the input of the change detection index.

### **Data-poor case study**

For Pakistan, two set of roads for the Muzaffarabad central district were delineated from Google Maps using polylines to represent primary and secondary roads. These were then manually adjusted using the vector editing function in QGIS to the co-registered images to account for positional shift between Google Maps and Google Satellite data. From a visual inspection of the satellite images, two thresholds of road width were identified: 4 m for primary roads and 2 m for

secondary roads.

As for the case of Van, the roads polylines were merged using the function Dissolve in QGIS and then split into 100 m long segments to be used as a consistent base for the analysis. Buffer distances based on the road width thresholds were applied to the 100m segments to include as much of the road surface as possible. Each buffer polygon was used to clip a single road segment off the pre- and post-event panchromatic and pan-sharpened images. The clip process was repeated for all the buffer polygons of both primary and secondary roads, to be used in the change detection index calculation.

For Pakistan, the available satellite imagery was pansharpened and co-registered to ensure spatial accuracy between the buildings extracted from the pre- and post-event images using the **Footprint Extraction** tool from the SENSUM QGIS toolbar. Visual inspection of the images allowed the identification of a series of buildings' roof colours typical of the Muzaffarabad area: red, white, grey, blue, light blue, yellow and brown. A training set based on the different roof classes and auxiliary ones, such as low and tall vegetation, water, roads and bare ground, was delineated in shapefile format, to be used as input parameter for the **Footprint Extraction** tool. The optional smoothing filter was applied in the tool settings, increasing the processing time for the entire scene up to 24 hours. If not used, the high spectral variability of the image could result in a higher rate of misclassification.

## Results



Figure 3.6 Pre-disaster QuickBird image of Kashmir, Pakistan, clipped by the buffered primary roads.

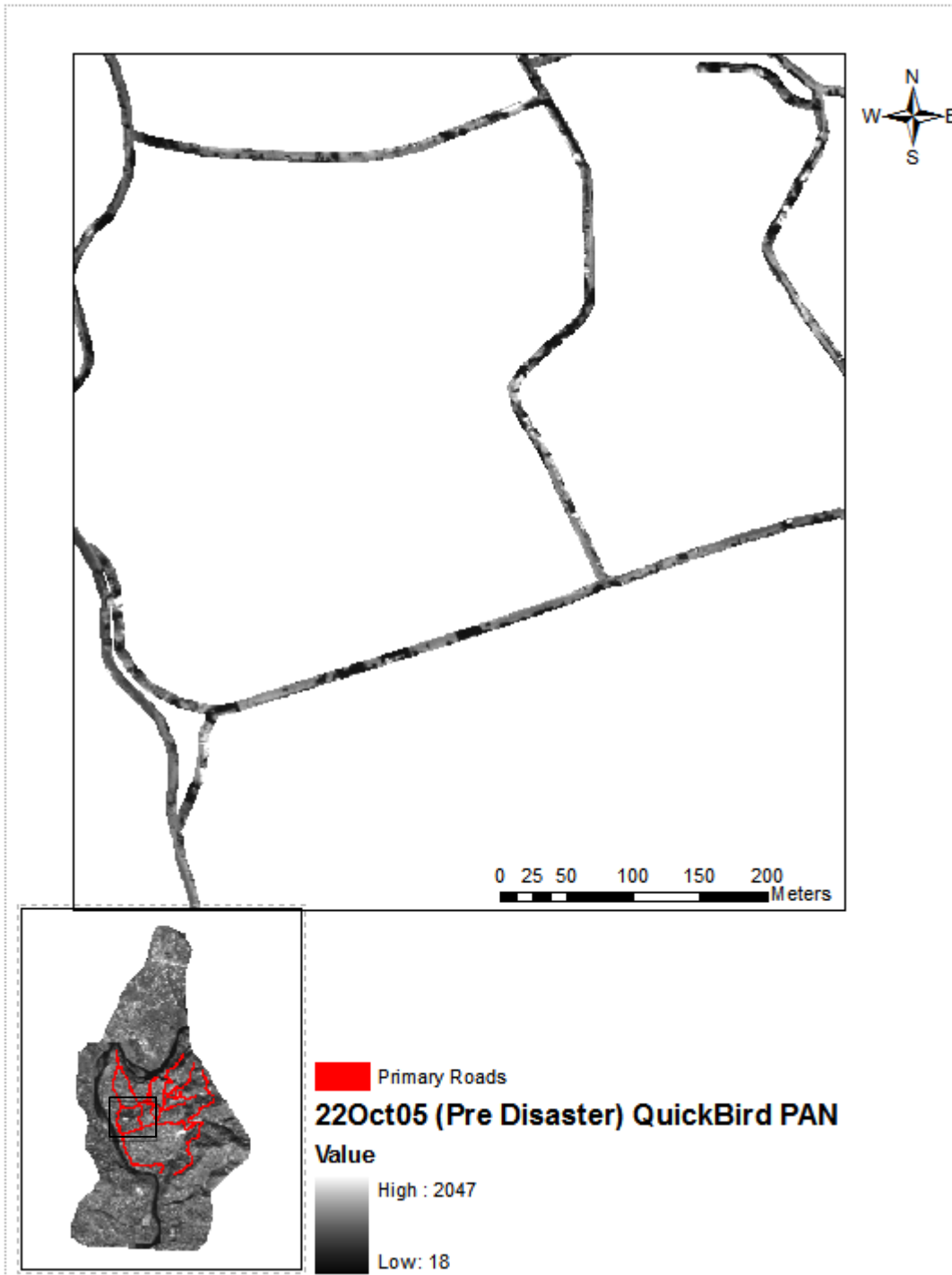


Figure 3.7 Post disaster QuickBird image of Kashmir, Pakistan clipped by the buffered primary roads. This image was taken 14 days after the earthquake.

Using the images shown in figure 3.7 and 3.8, Normalized difference of the gradient, edges, and roughness are calculated for the PAN bands and PAN sharpened Infrared bands.

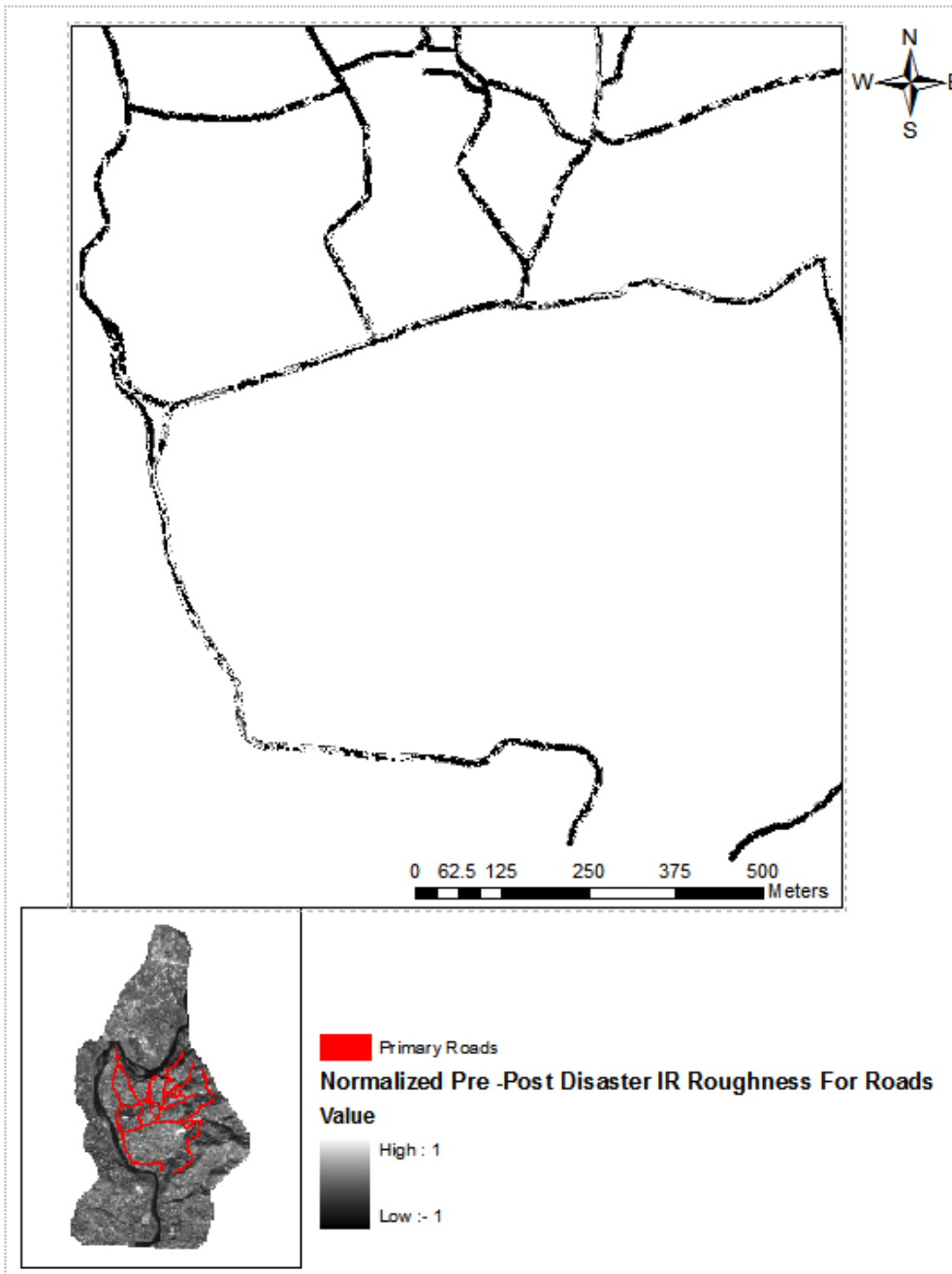


Figure 3.8 The Normalized roughness difference between pre- and –post-PAN images pertaining to the primary roads.

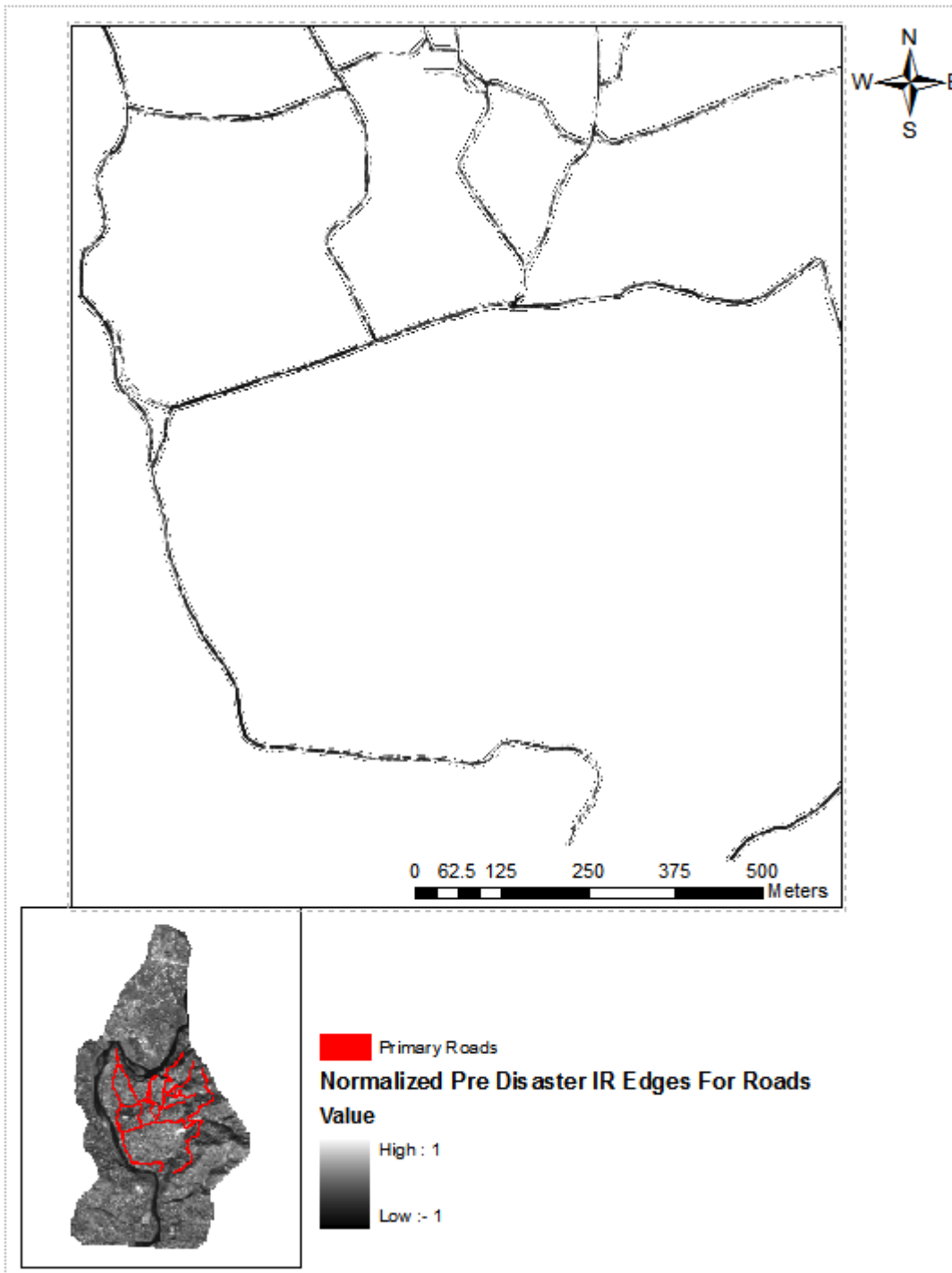


Figure 3.9 The Normalized difference in the edges between pre- and post-infrared images pertaining to the primary roads.

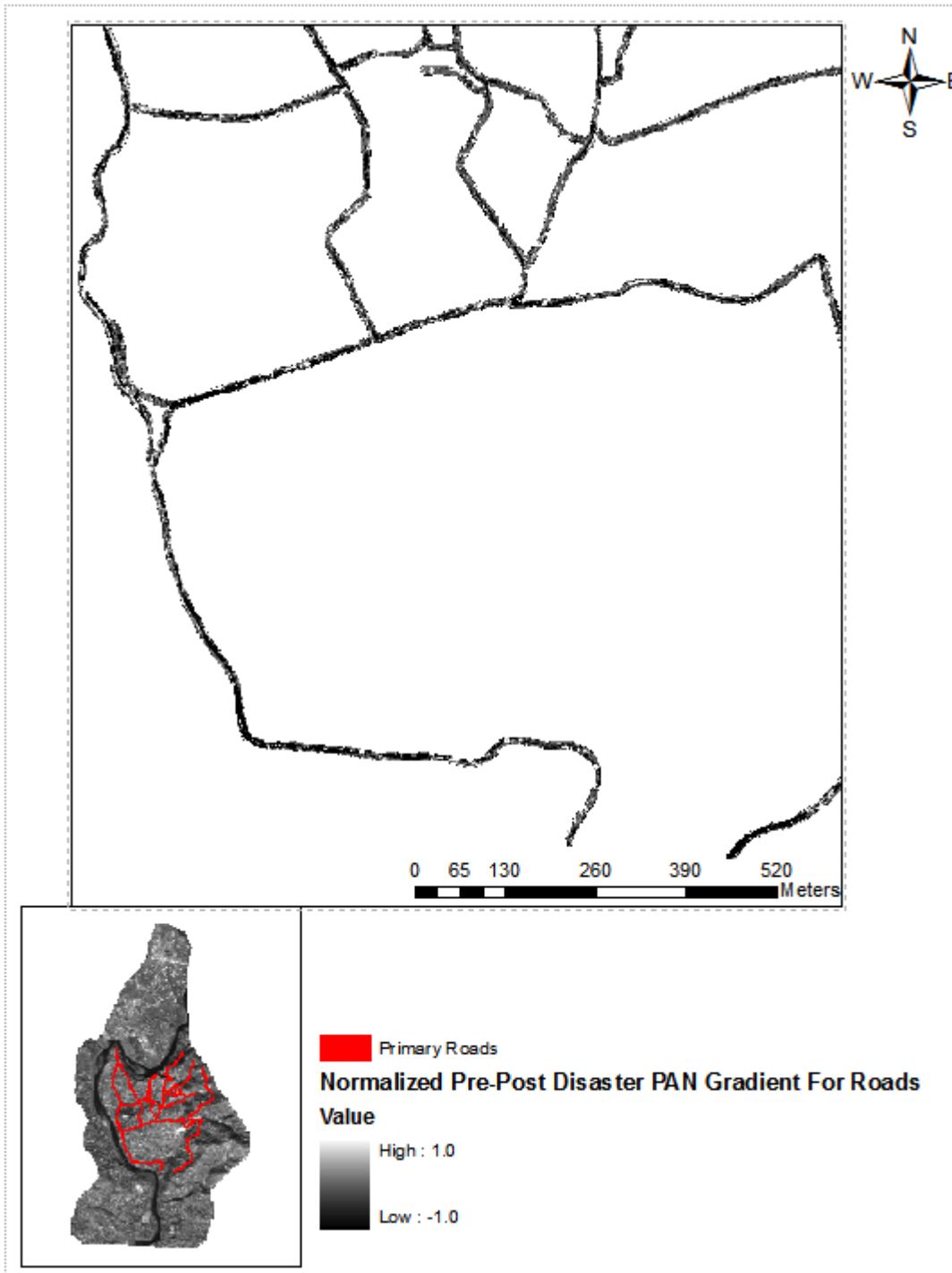


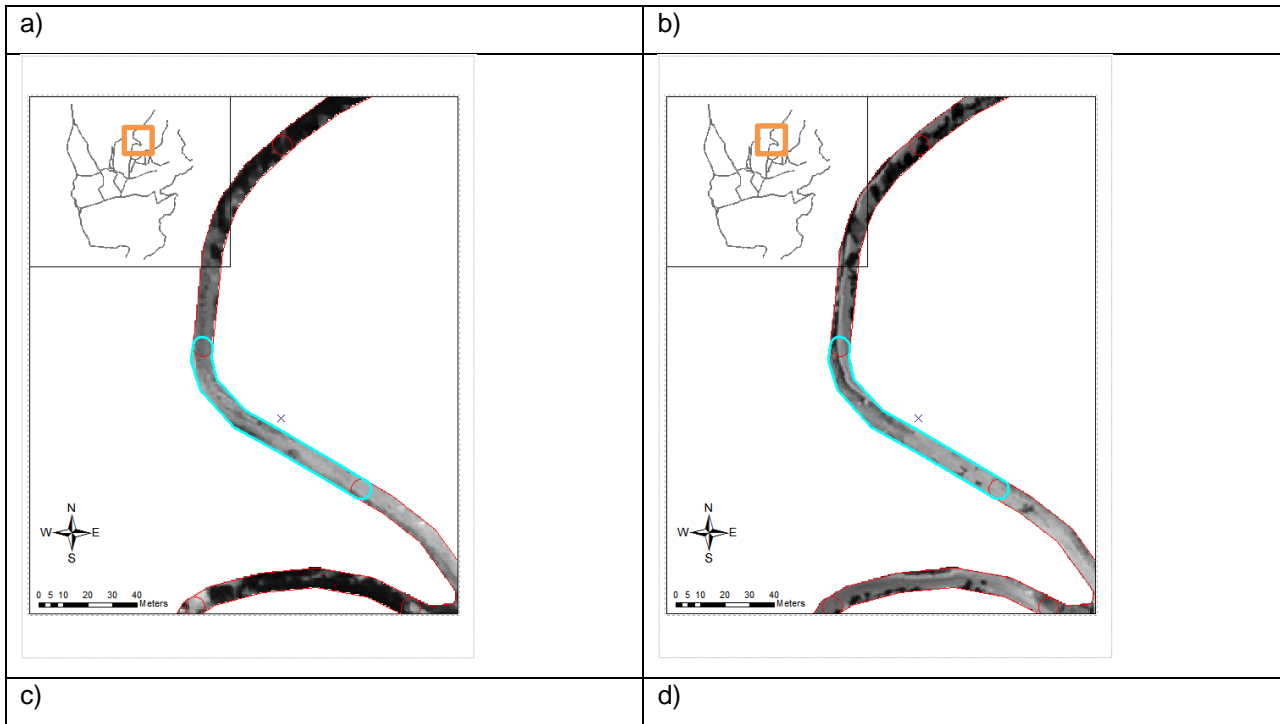
Figure 3.10 The Normalized difference in the gradient between pre- and post-PAN images pertaining to the primary roads.



The normalized pixel values are averaged across each buffered road segments to obtain an average change in roughness, edge and gradient.

### Visual Index

Using the pre- and post-images, a visual index between 0 and 9 was determined. This visual index is regressed against the Normalized differences of the gradient, edges and roughness to get the coefficients to combine the combine the normalized differences to form an Enhanced Change Detection Index.



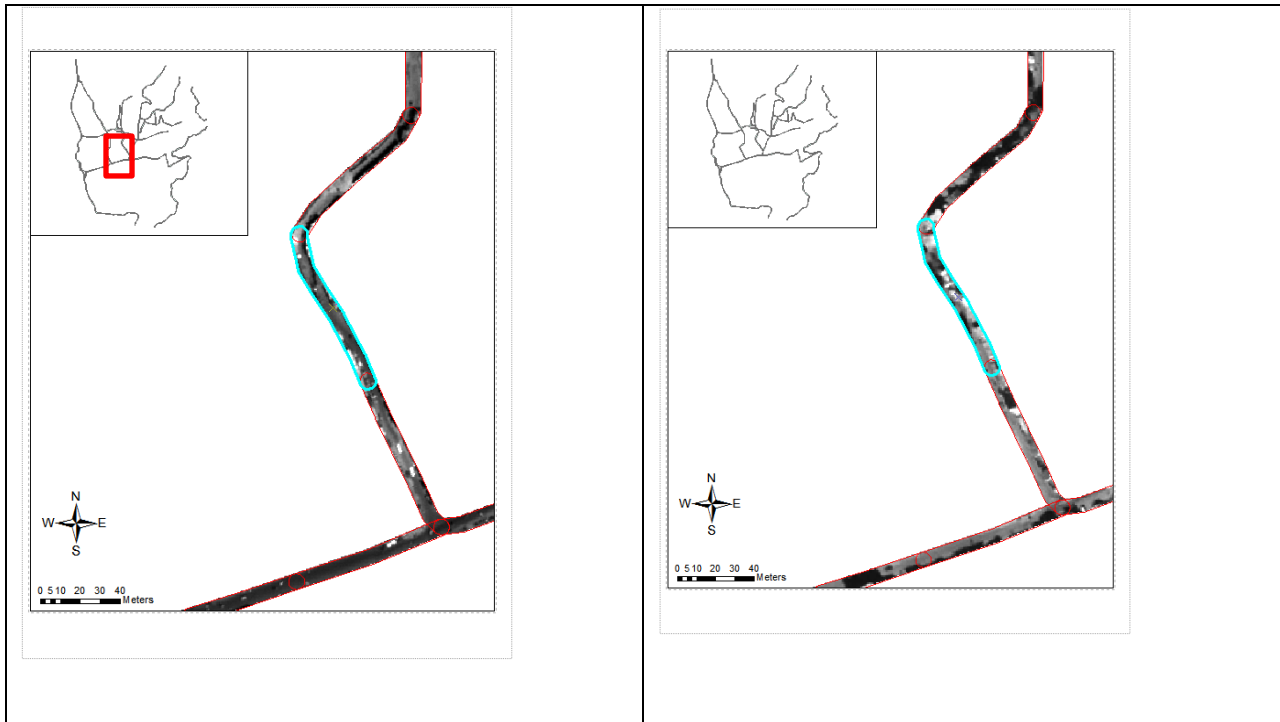


*Figure 3.11 a) and b) are the pre- and post-images of the clipped roads. By looking at these images, a visual index of 2 was determined because the roads have not changed much between the two images. C) and d) show a considerable change, hence a value of 9 is used as the visual index. 30 road segments were visually analysed and an appropriate visual index determined*

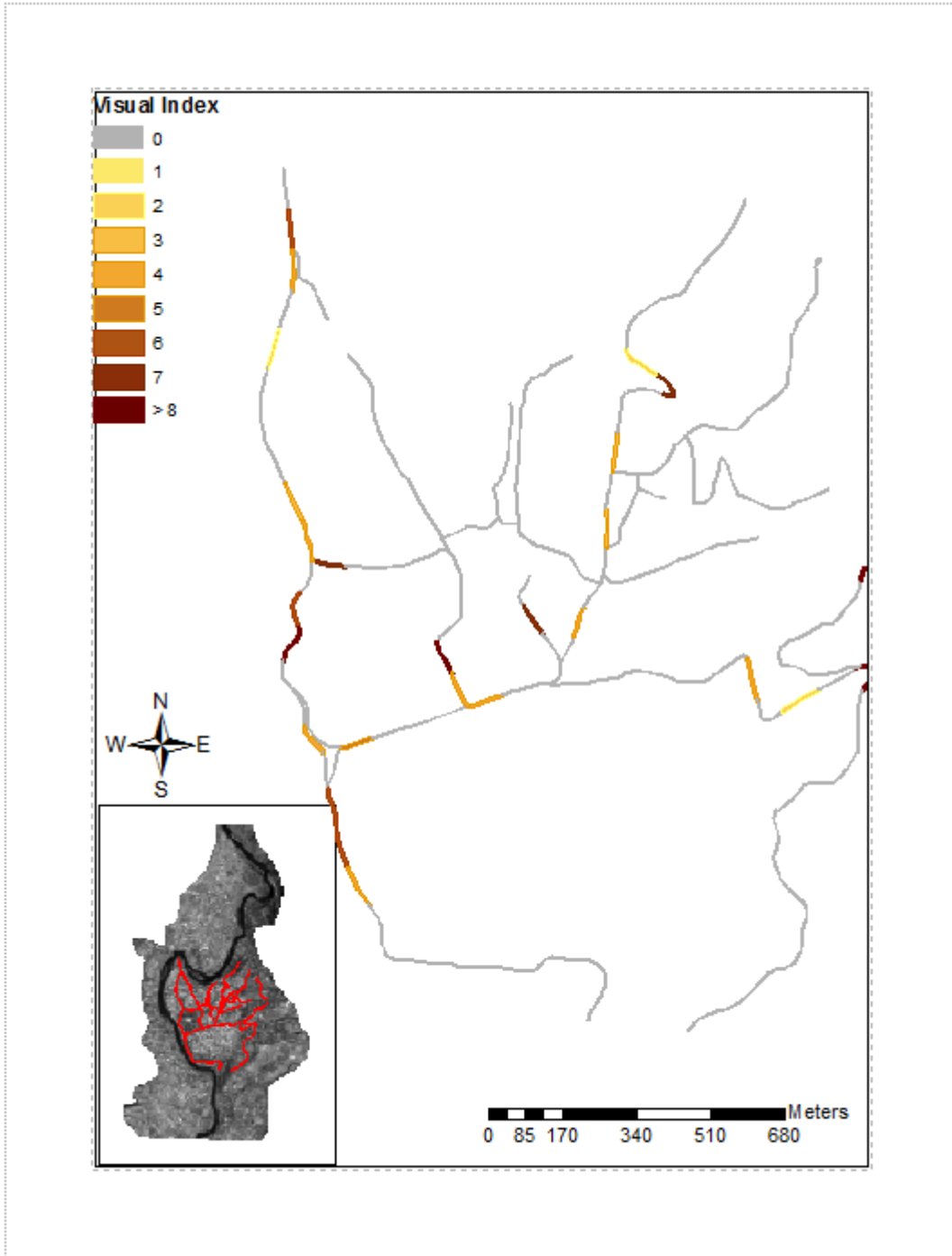


Figure 3.12 The visual index for randomly selected road segments are shown in the above figure.

The visual index, the derived normalized gradient, edge and roughness parameters and regression coefficients are used to come up with an Enhanced Change Detection Index.

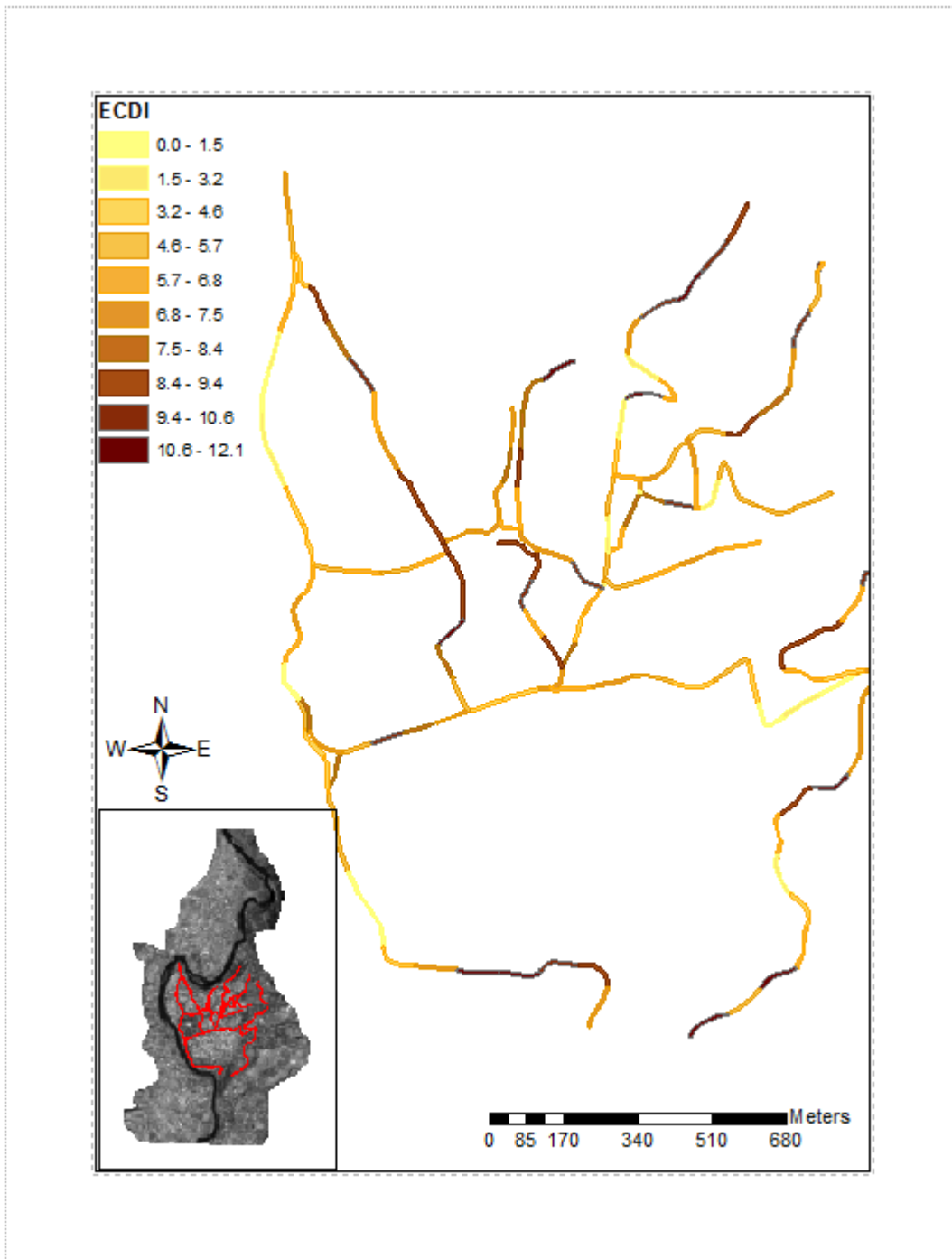


Figure 3.13 The Enhanced Change Detection Index is shown for all the roads. This is an indicator of degree of change between the pre- and post-disaster images.

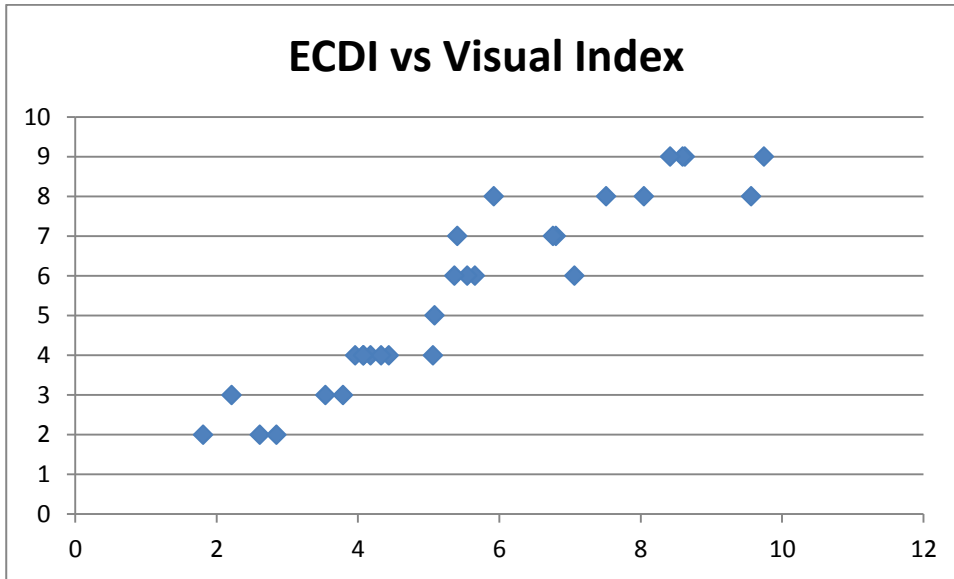


Figure 3.14 Visual Index vs. Enhanced Change Detection Index(ECDI) for all the roads. Visual Index and ECDI show a linear relationship for the roads.

### 3.3 Camp Detection Tool

Tents can be used as being representative of numbers of refugees and the accurate estimates of refugees can be inferred from the number of the tents. Tents are typically very small and have definite shapes and sizes. The typical way to count tents is in situ assessments provided by the local or international NGOs in charge of setting up the camps. The method can obtain very detailed information about the tents such as whether they are occupied or not. However, the in-situ assessments of the number of tents and therefore the number of refugees are time consuming and can perhaps be biased. Mainly due to the availability of very high spatial resolution satellite sensors such as Ikonos-2, QuickBird, Orbview-3, IRS-P6 and EROS A&B (Bjorgo 2000a), extracting tent-related information from satellite imagery is recommended.

There has been little research specially focusing on automation. Most ‘methods’ use visual tools to identify the camps (Giada et al., 2003; Bjorgo, 2000b). There are issues with a pixel-based classification method, for example, tents were wrongly assigned as grassland, if the camp is surrounded by grassland. It was therefore shown to have a low overall accuracy, as the contrast between the spectral values of tents and grass are not distinct enough.

### 3.3.2 Method

Before one begins to investigate the possibility of automated methods for camp detection, one must first set the rules for the physical recovery indicator- what makes a camp? What rules need to be in place to filter out camps from other urban built up and other damaged areas?

Tents have a regular building structure and has distinctly different spectral and texture from urban buildings. The characteristics we can therefore use to identify these automatically with a computer are spectral, spatial (area and shape), and texture (compactness and smooth).

Almost all the reviewed research uses object-based segmentation and classification employing the commercial Ecognition software. Within SENSUM, the ambition was to use only public open source software and therefore these made up methods explored in this work package.

The Joint Research Centre of the European Commission (JRC) hosts an Emergency Management Service which provides two products in rush mode and non-rush mode to disaster management. Their recently developed object-based segmentation and classification with mathematical morphology are reported to give good performance in detecting refugee camps (Giada et al., 2003), therefore, it was decided that these methods would be explored further for the WP5 workflows for recovery evaluation and monitoring.

Currently, there are four methods to detect camps: visual analysis, the pixel-based classification, the object-based segmentation and classification, and the mathematical morphology. The visual analysis is therefore always used as reference scenarios and used to assess the accuracy. The pixel-based classification makes use off-spectral characteristic to identify objects such as tents. It is relatively simple and can be implemented easier. Almost all remote sensing software has provided such functions. It can be further distinguished as supervised and unsupervised classification. The supervised classification needs the user to provide training data before classifying the image. Naturally, supervised classification performs better than unsupervised. However, the method deals with only pixels. Due to the changing spectral reflection, some pixels will be wrongly assigned to other objects. The object-based segmentation and classification includes two stages: multi-scale segmentation and fuzzy logic classification. This kind of classification is based on objects rather than pixels and is expected to have better performance than pixel-based classification, but is more complicated to implement. In addition, it would be

difficult to obtain the open-source library. Similarly, as commercial software like Ecognition was used to derive these methods, it will be difficult to obtain the detail technique behind the algorithm or to mimic this.

The fourth method is the mathematic morphology. This method is especially useful for objects characterised by the clear shape, size and contrast. It uses the morphological erosion and morphological dilation to identify targeted objects such as tents. UCAM developed an automatic mathematic morphology method to identify the tents. The method includes four steps: morphological opening, opening by reconstruction, top-hat by reconstruction, morphological threshold.

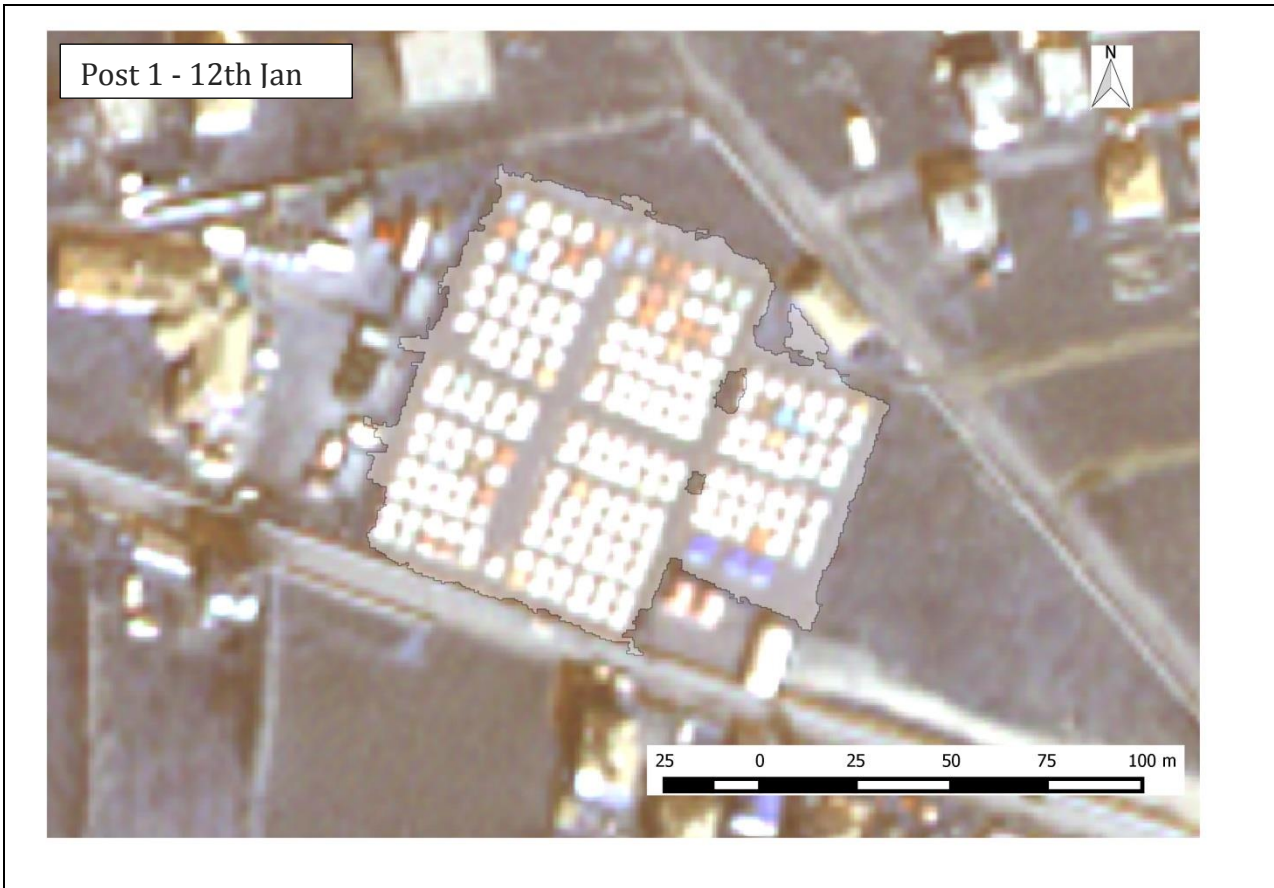
For the case study of Van, the method has been tested on a camp area which was automatically detected with the open spaces workflow.

The corresponding area has been clipped from the Post 1 (Figure 3.18) Image, acquired 2.5 months after the quake and extending over the northern portion of the area of Van.

As seen in Figure 3.18, the area was unoccupied by camps in the pre-image, shows the presence of camps in the Post 1 image, but all the tents had been removed before the acquisition on the Post 3 image WV02 image on 5<sup>th</sup> June 2013.







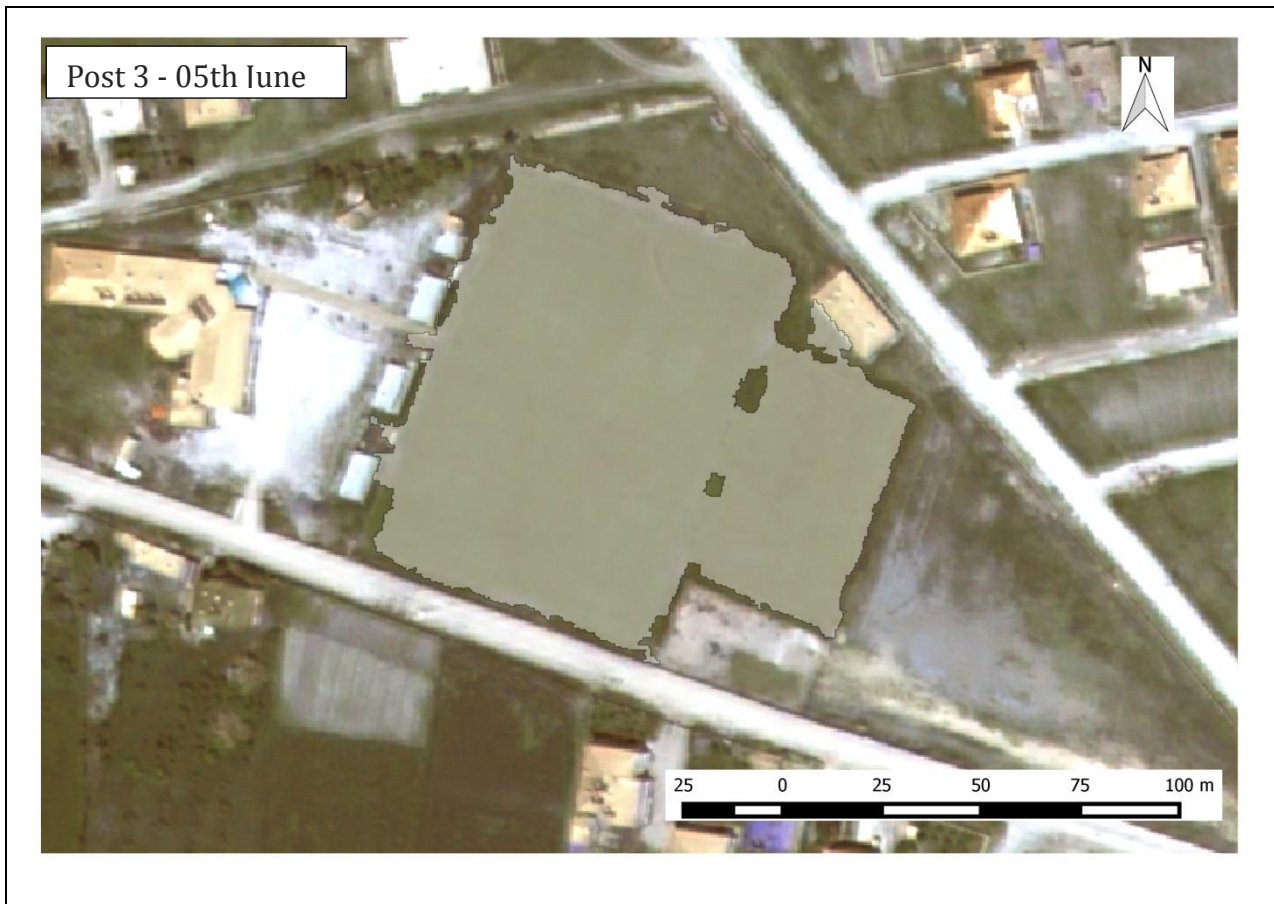


*Figure 3.15 Evolution of a camp site over the time period from the acquisition of the pre-image and the Post3 (recovery) image. The Post 1 image shows the existance of camps while the Post 3 show camps being removed.*

The camp area has been analysed with the mathematical morphology algorithm, which requires the user to input tent sizes and thresholds. Several combinations of these two variables have been tested and the best combination is presented in Figure 3.19, in which both tent size and threshold are set at 0.5 m. The result has been then polygonised to obtain from the output raster a vector product to allow for the automatic counting of the tents.

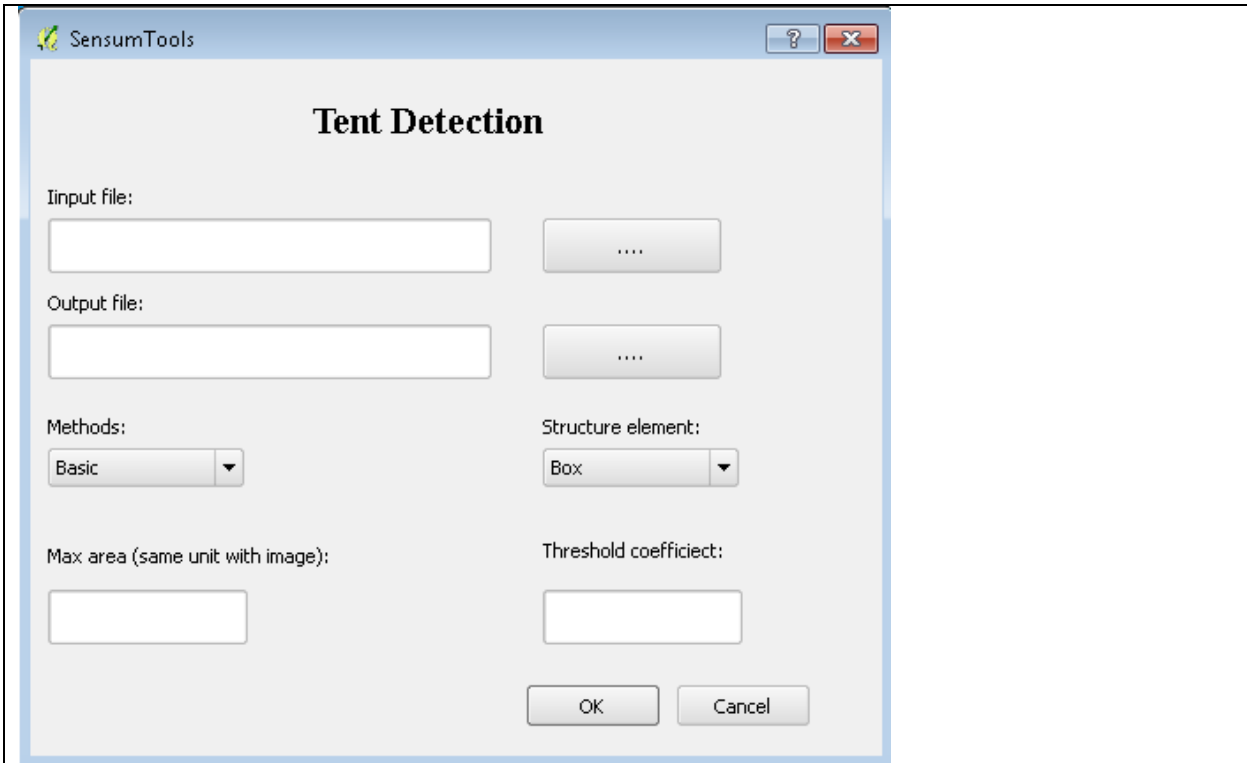


*Figure 3.16 SENSUM plugin for camp detection. Several combinations of the two variables (max area and Threshold coefficient) have been tested.*

It can be easily noticed that the great majority of tents are identified by the algorithm with few duplication errors, in which more than one polygon is superimposed on a single tent. The tent count has been implemented automatically with polygon to polygon intersection, which essentially count the number of polygons falling into the boundary of the designated camp.

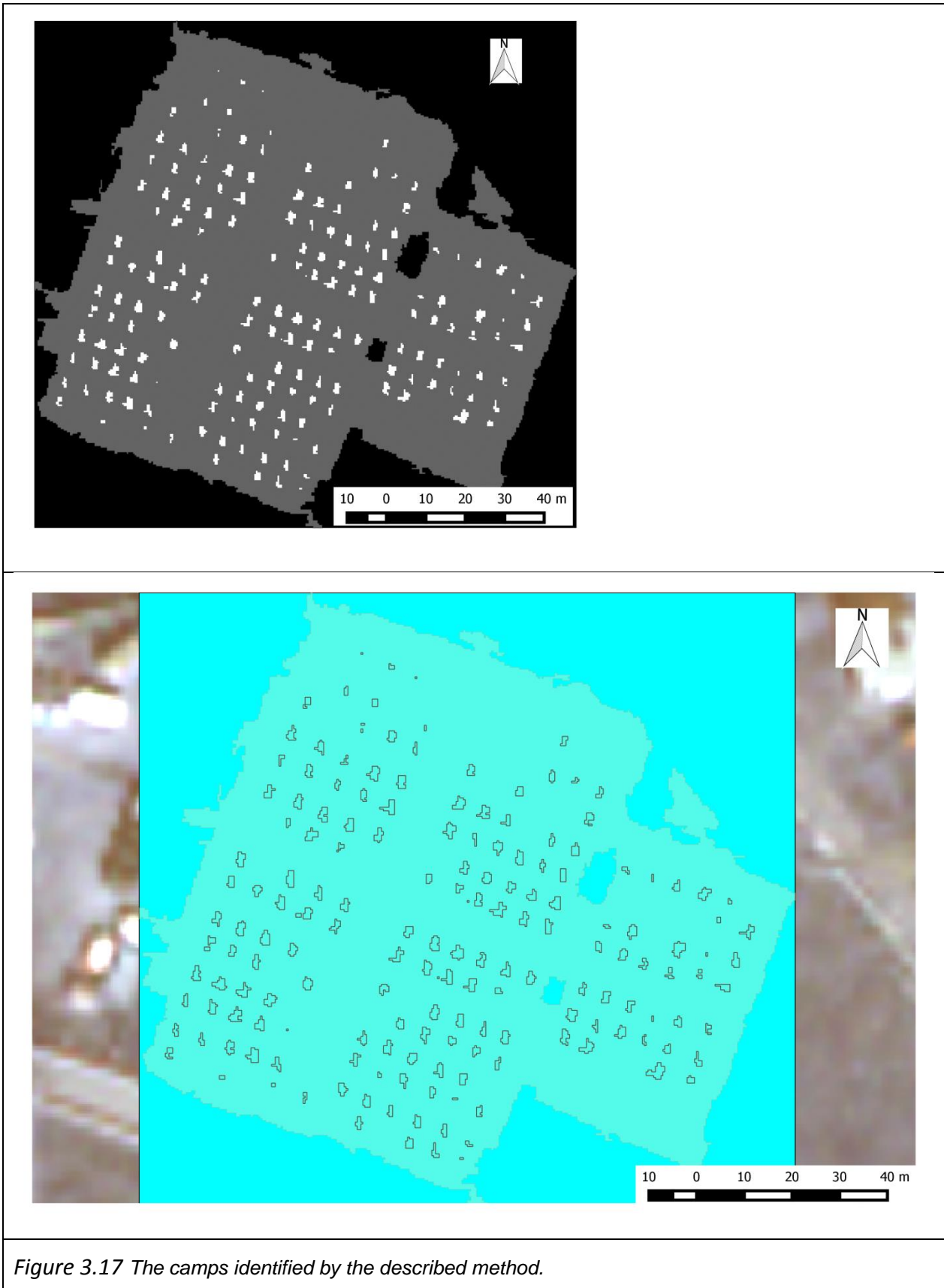
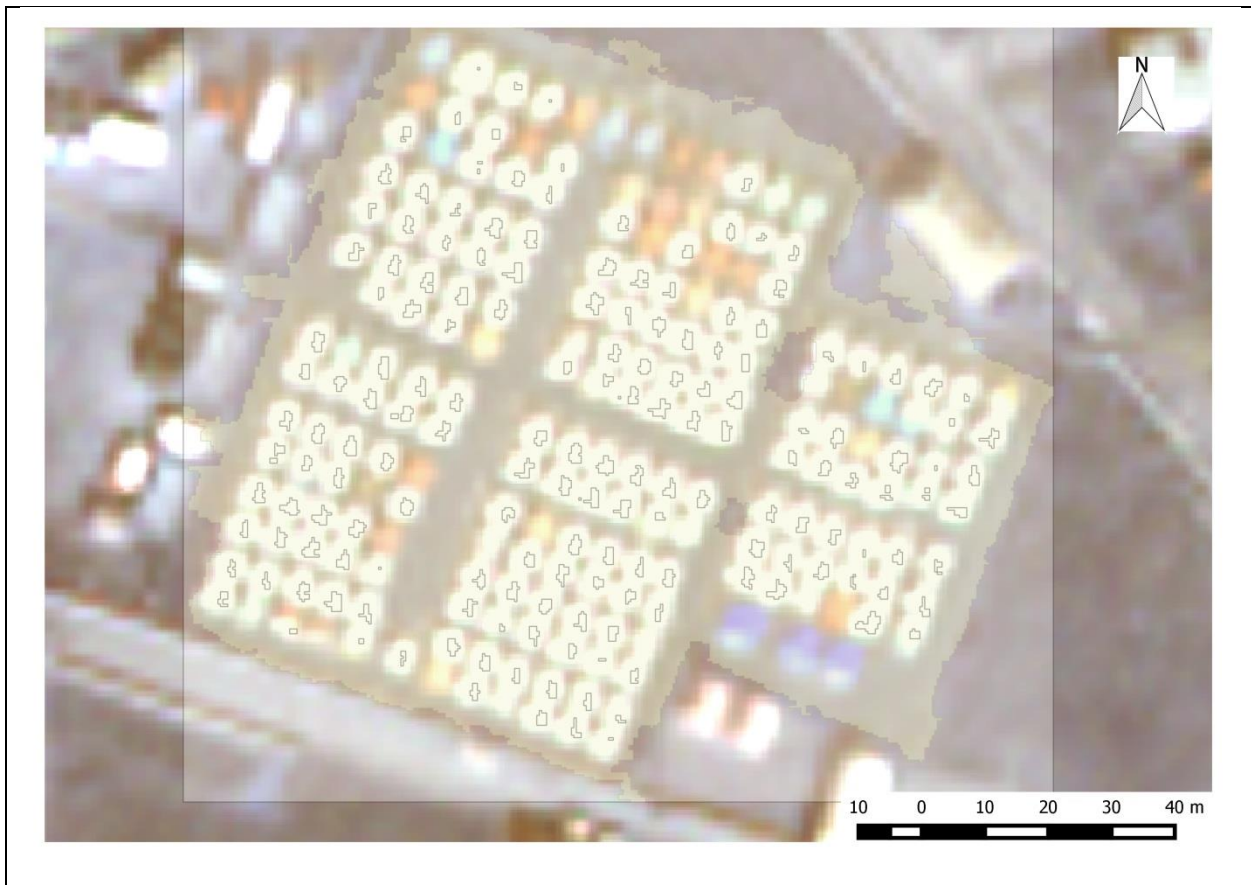
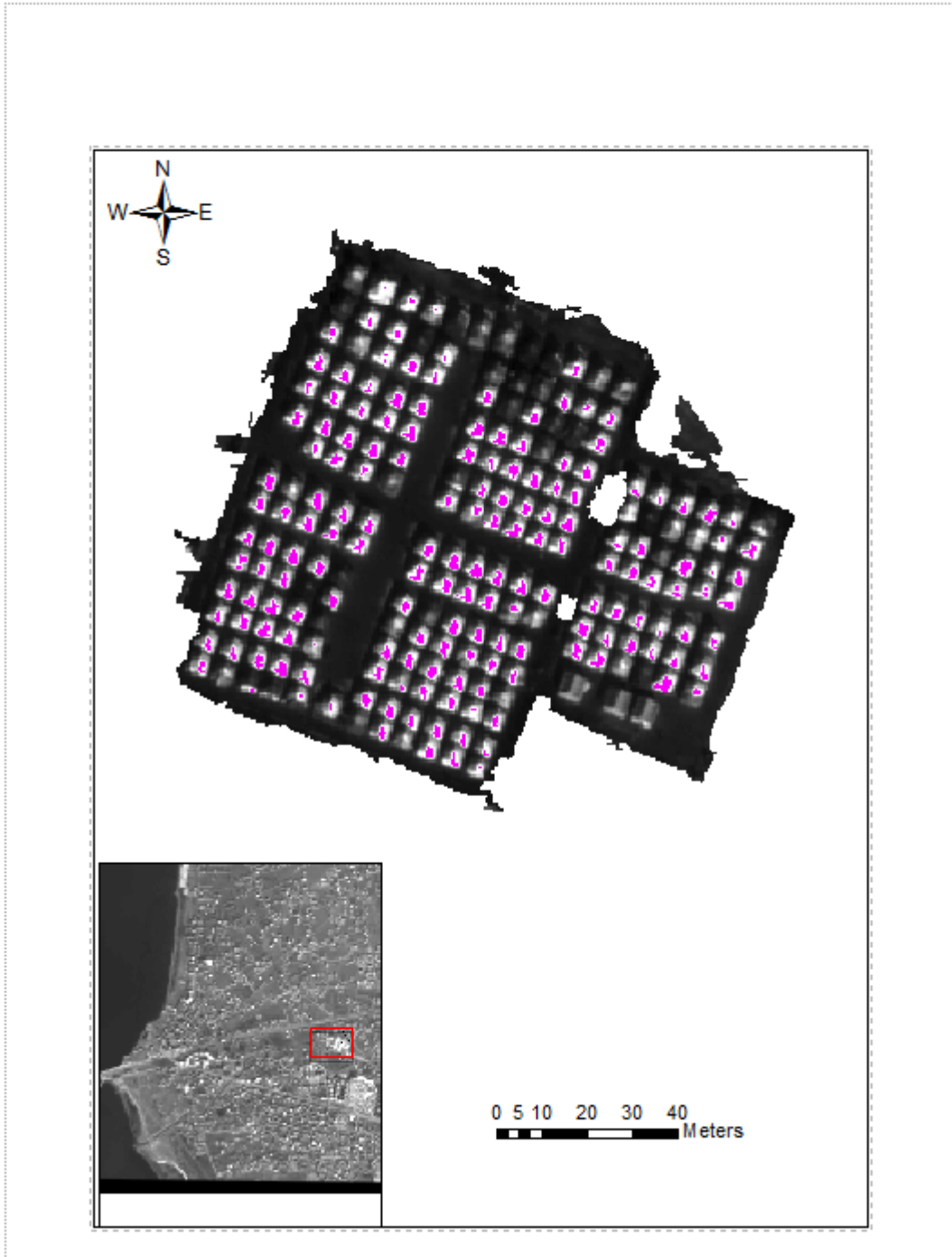


Figure 3.17 The camps identified by the described method.

Of a total number of 209 tents, only 33 were unclassified, giving a false negative error of less than 16%. Only 6 out of 209 tents were counted twice, giving a false positive error of 0.02%. Overall, the number of tent correctly identified was 170, giving more than 81% accuracy (Figure 3.21).



*Figure 3.18 The distribution of automatically extracted tents polygons on the input image.*



*Figure 3.19 The camp detection function based on image morphology was tested at an open space in Van, Turkey. The camps detected from are shown in purple.*

### **3.4 Open Spaces Assessment**

The location and size of open spaces is a very important requirement both in early-recovery and during the monitoring and evaluation phase. In the early phases of emergency response and rehabilitation, the location and size of open spaces is of interest for emergency managers looking to find the best plots for camps. In the monitoring and evaluation phase, knowing the locations of camp areas is essential to understanding and monitoring the rehousing of the population and the change of use of the previously occupied camp areas. It is important to note at this stage that a number of other factors besides the size of the camp contribute to the choice of a specific area over another. Such factors may include, for instance, hazardous site locations, existence of communication links that allow for the area to be easily restocked in supplies, and the proximity of other services such as hospitals and schools.

The method proposed here is area-based. Nonetheless, the workflow proposed in 2-E and here in Figure 3.23 can be modified to introduce other control elements. The method is used as a stand-alone method for the identification of open spaces of a chosen affected area or as a module to be run before the camp analysis to isolate open spaces of suitable area for camp allocation, thus reducing commission errors of the tent count described in section 3.3.

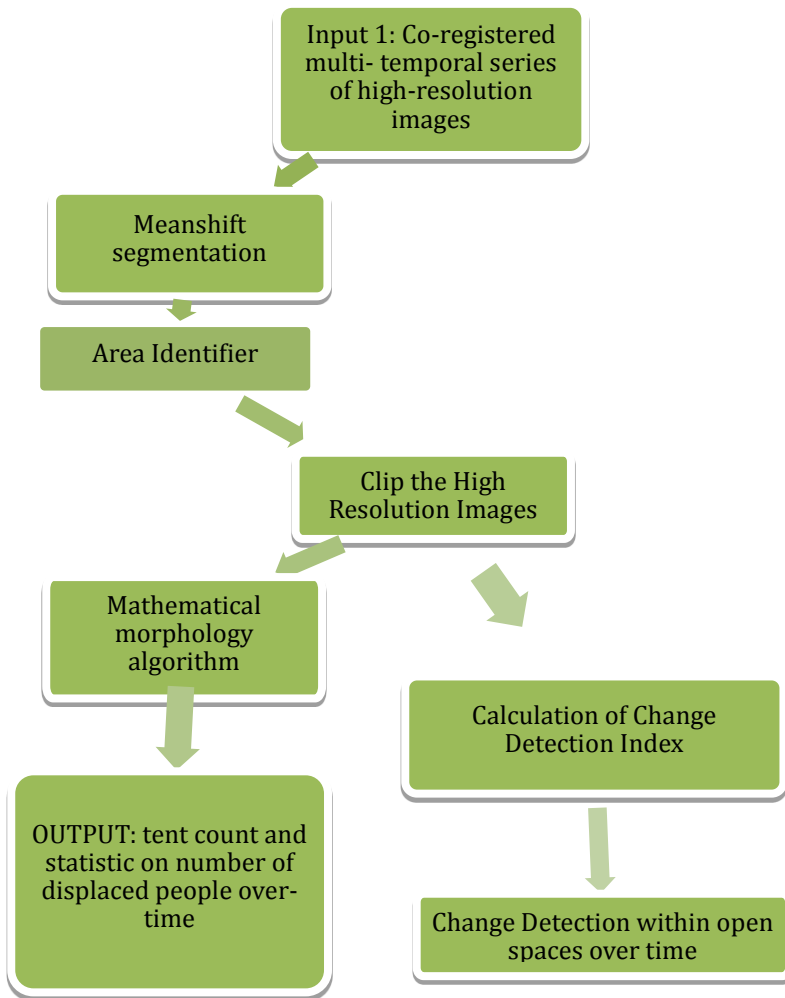


Figure 3.20 Workflow of the open area detection and detection of camp grounds.

As shown in the above workflow, this method has as input the co-registered panchromatic and multispectral satellite images acquired for each of the case studies.

Following the same rational applied in the accessibility workflow, in order to detect local changes, the change detection index is applied to the same portions of an image in the time series. Each of the portions represents an open space which has been detected by segmenting the pre-disaster panchromatic image using a Meanshift segmentation algorithm available in Orfeo Toolbox in QGIS as well as part of the SENSUM plugin for QGIS. The area is then calculated for each of the segmented parts of the vector file resulting from the segmentation. Based on visual inspections on the areas occupied by camps, a range of areas was defined to extract from the segmented vector scene only those segments whose area may be suitable for the allocation of camps. Each of the images of the temporal series is then clipped to obtain a series of open spaces images labelled



with a unique identifier.

For both Van and Muzaffarabad, the lower and upper bands of the threshold were chosen by means of visual inspection by looking at what areas had been occupied by camps in the post-disaster image and of these detecting the corresponded divided segments to calculate the areas. For the specific case of Van, the selected areas ranged from 10,000 and 50,000 m<sup>2</sup>. The segmentation was accomplished using the Meanshift Orfeo Toolbox algorithm.

For the city of Muzaffarabad, the panchromatic pre-event image was segmented using the Meanshift segmentation algorithm, part of the SENSUM plugin for QGIS. The standard set of settings for the algorithm was used. The area of each segment was calculated using QGIS and a selection based on areas ranging between 1000 m<sup>2</sup> and 10,000 m<sup>2</sup> was used to extract polygons big enough to be suitable open spaces for, for example, setting up camps. Each selected polygon was used to clip a single open space off the pre- and post-event panchromatic and pan-sharpened images. The clip process was repeated to detect all the open space polygons.

### **3.4.3 Results**

The open spaces obtained from segmentation of images for Van, Turkey are shown in figure 3.24



*Figure 3.21 Open Spaces for Van Turkey are shown in green and are overlaid on a GeoEye image of a greater extent.*



Figure 3.22 Zoomed in version of a pre-disaster image showing the open spaces.

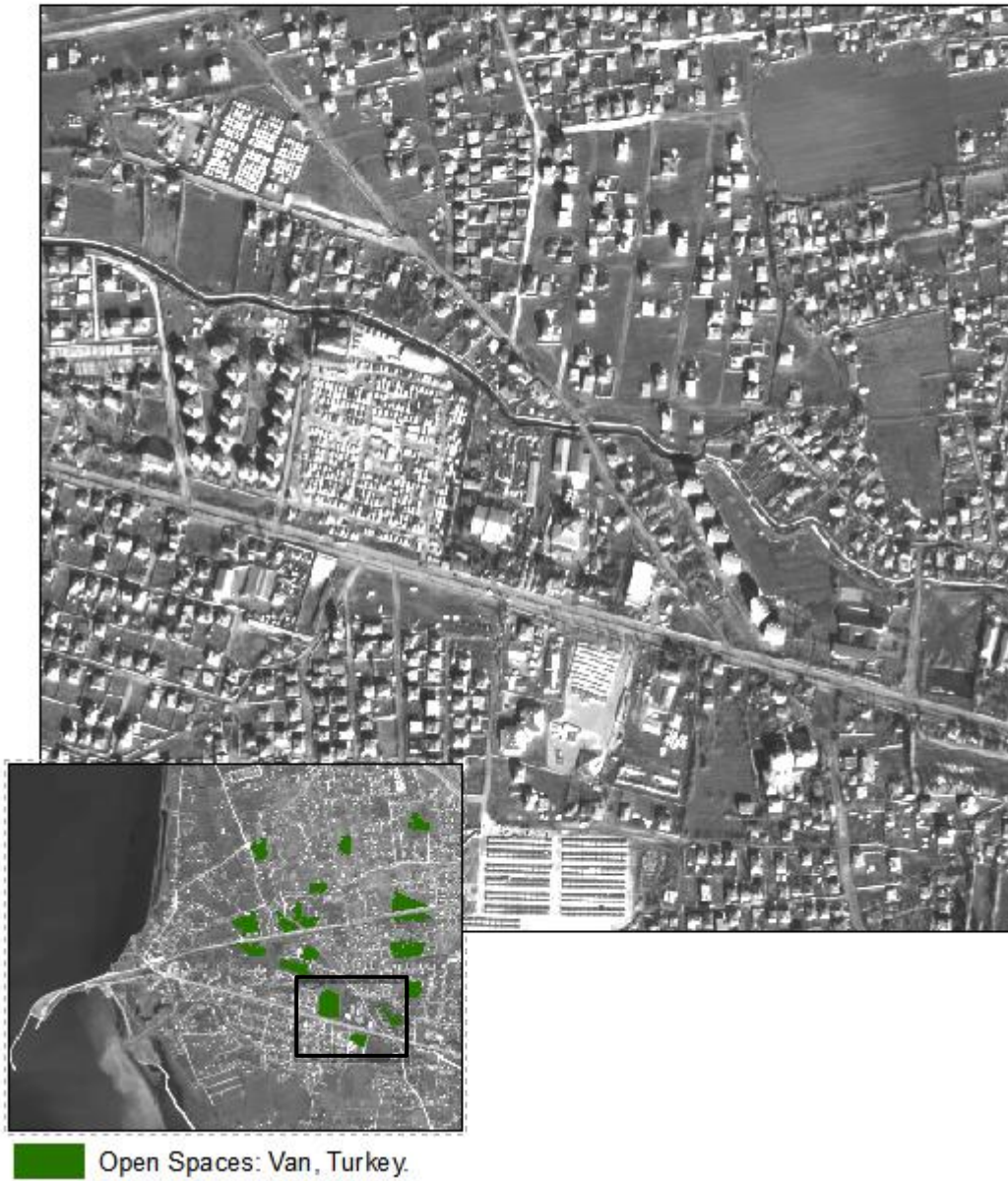
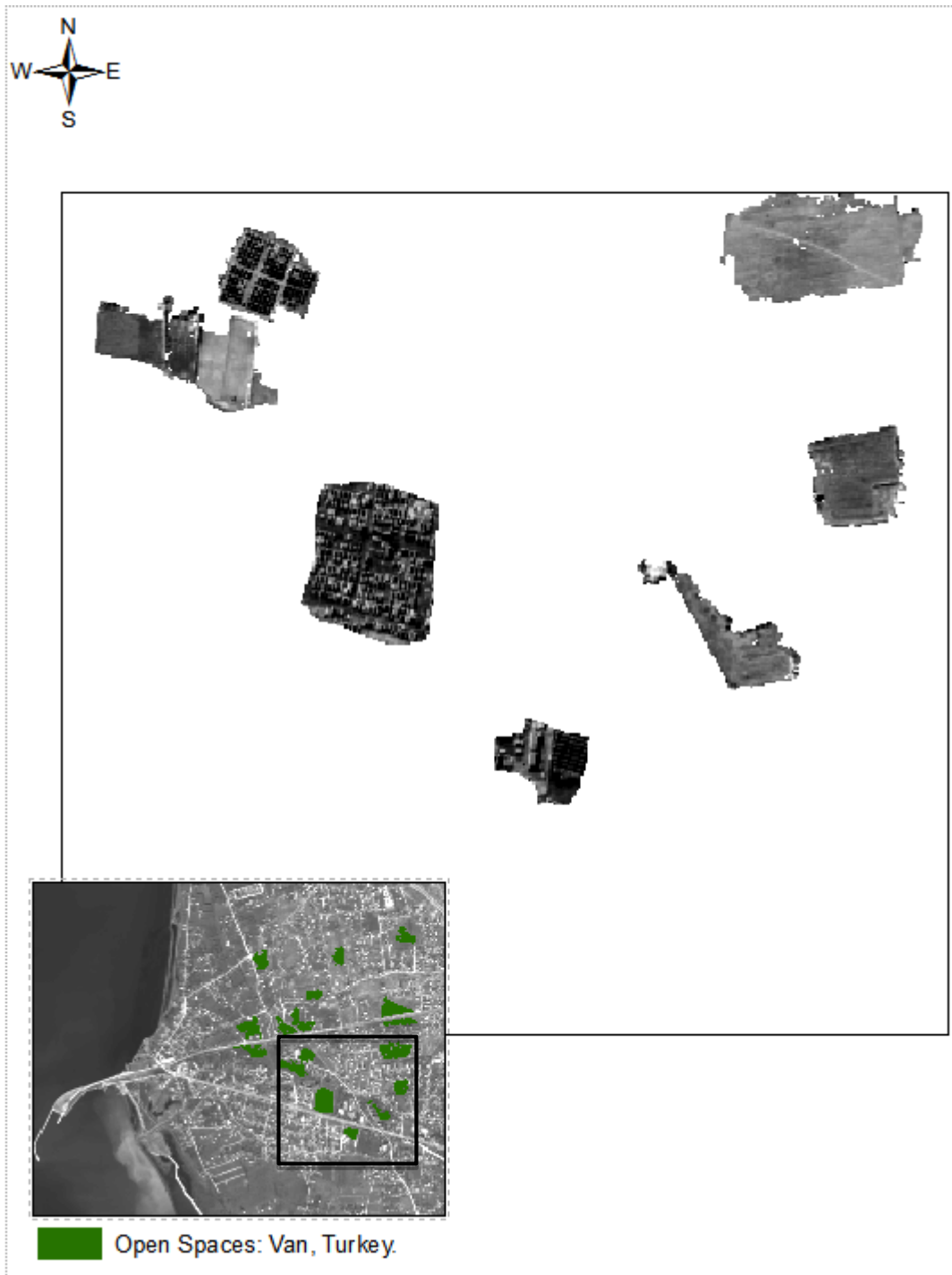


Figure 3.23 Zoomed in version of a post-disaster image showing camps in the open spaces.



*Figure 3.24 Normalized difference between the pre- and post-images pertaining to the open areas only. The open areas with camps show more texture than those areas with none.*

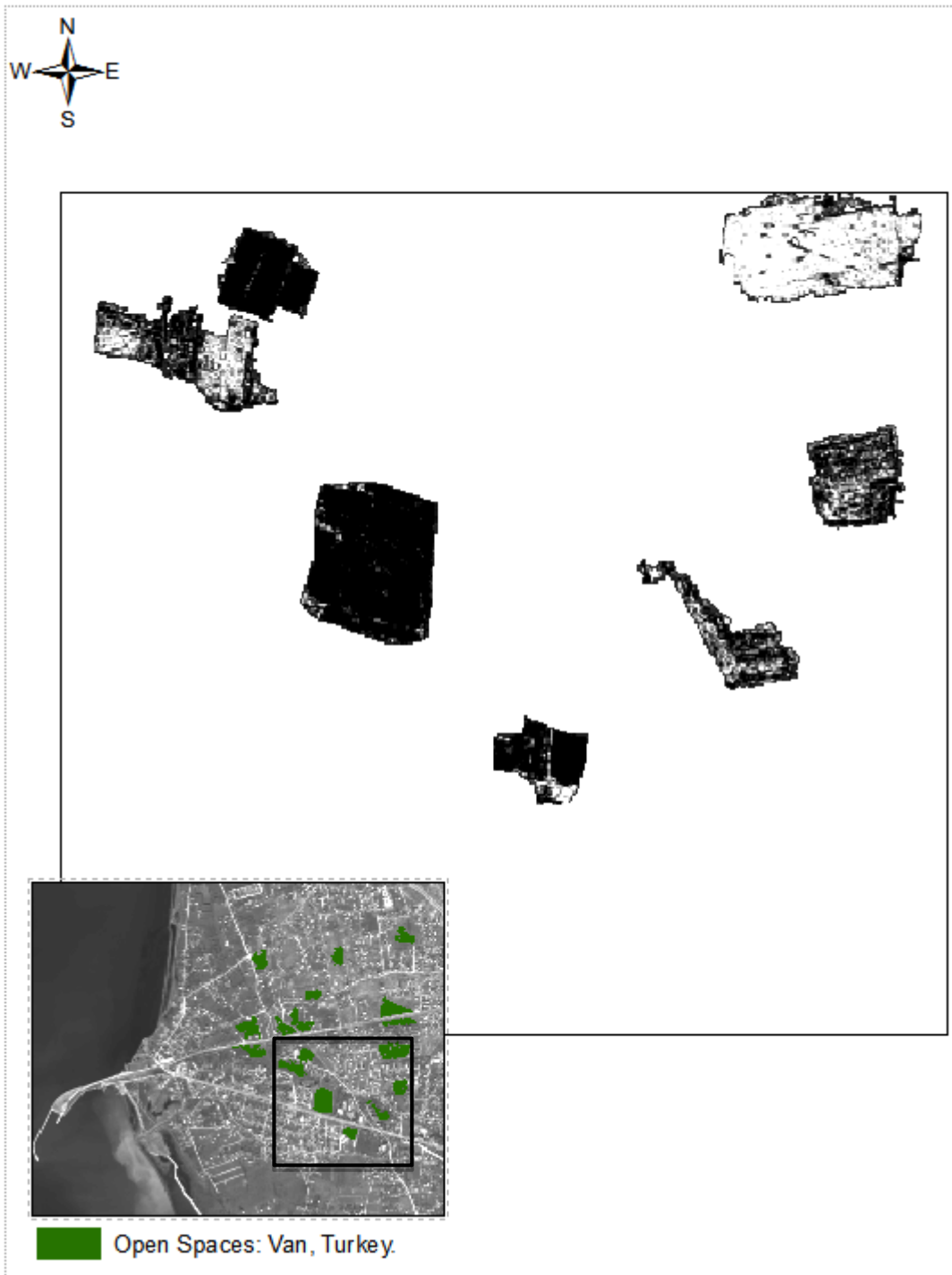
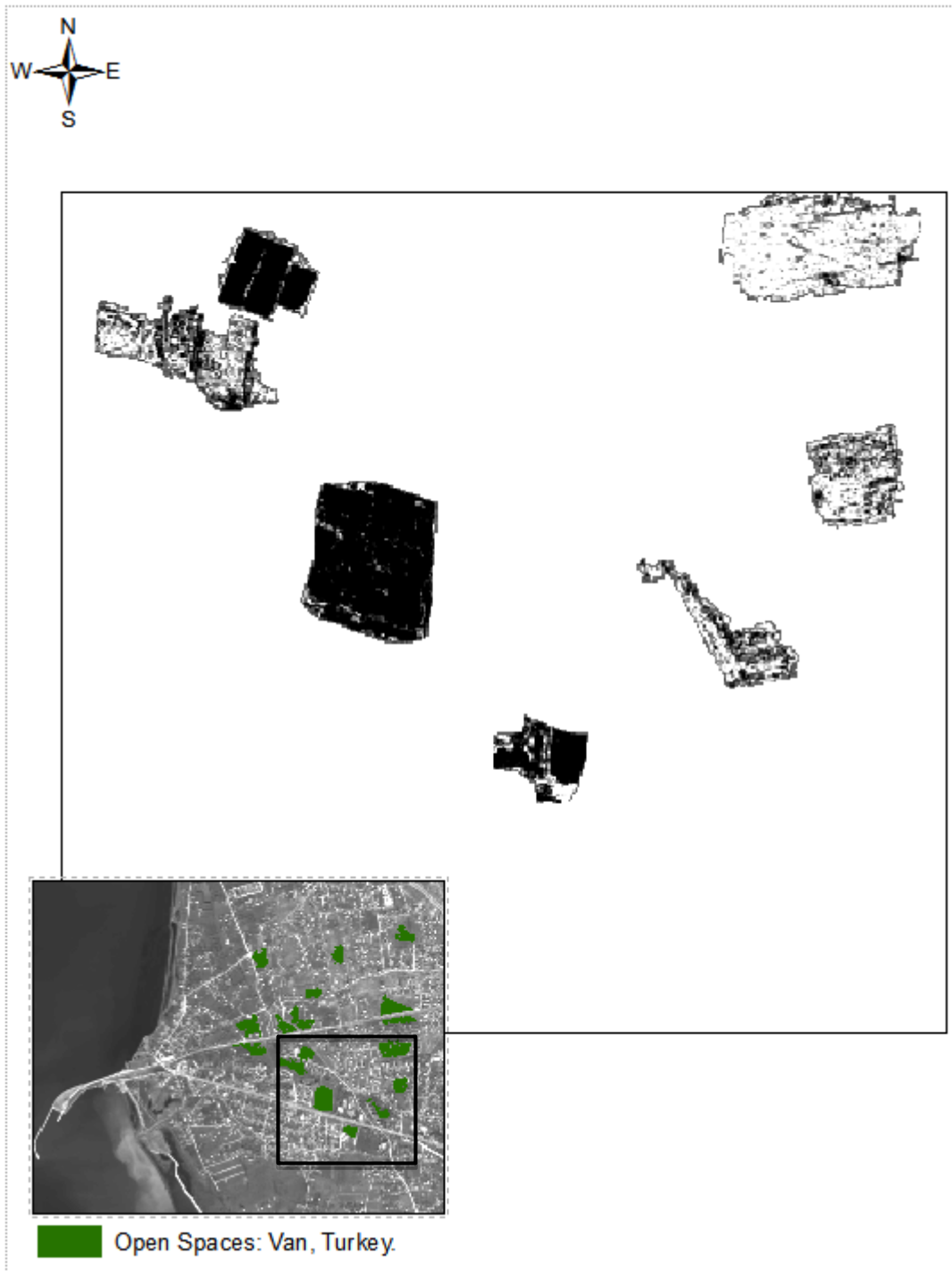


Figure 3.25 The Normalized difference of the edges with the open spaces.



*Figure 3.26 Normalised difference of the gradient within the open spaces.*

The normalized pixel values are averaged across each open spaces area to obtain an average change in roughness, edge and gradient.

## **Visual Index**

Using the pre- and post-images, a visual index between 0 and 9 was determined. This visual index is regressed against the Normalized differences of the gradient, edges and roughness to get the coefficients to combine the normalized differences to form an Enhanced Change Detection Index for the open spaces.



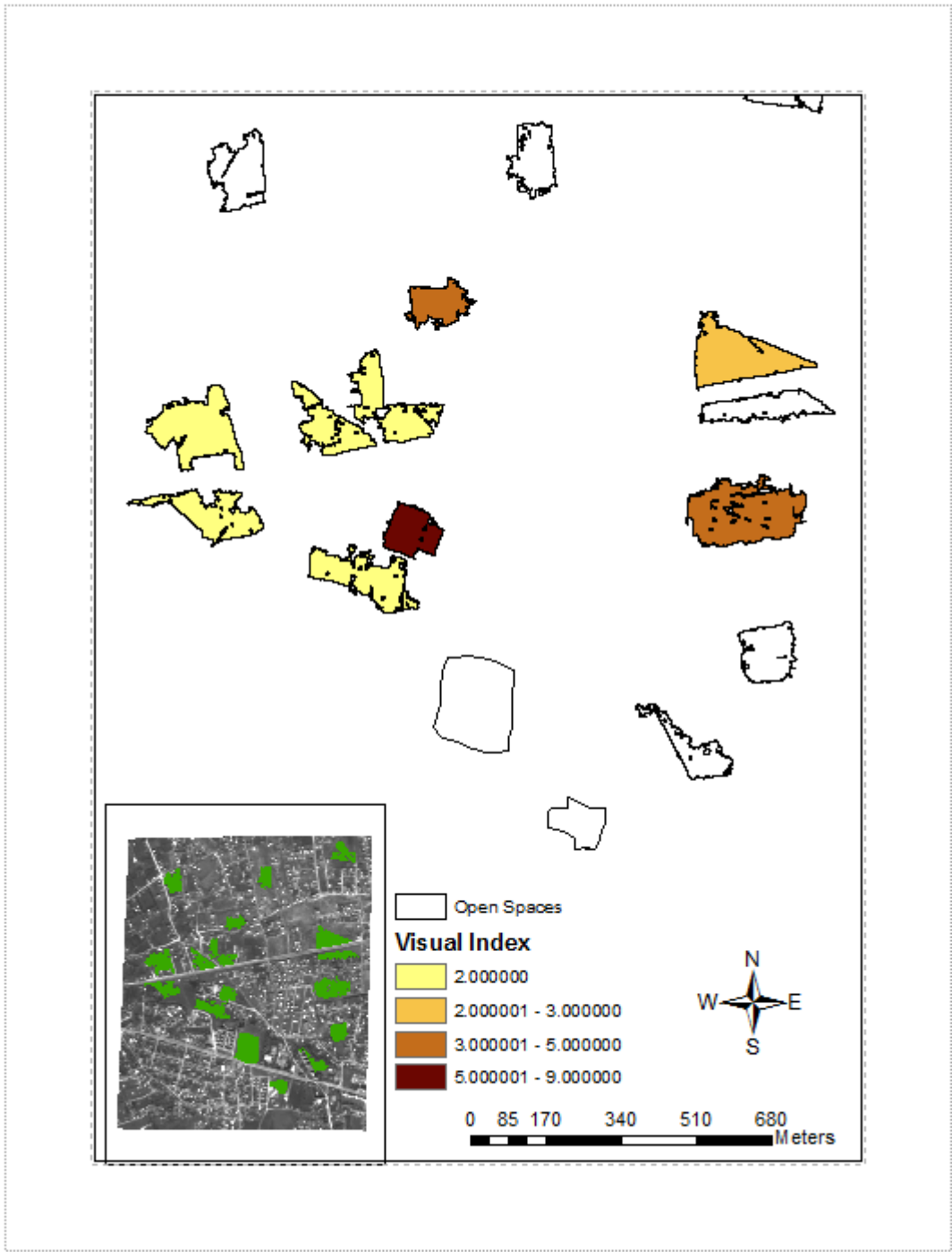


Figure 3.27 The visual index obtained from looking at the pre- and post-images of the open spaces.

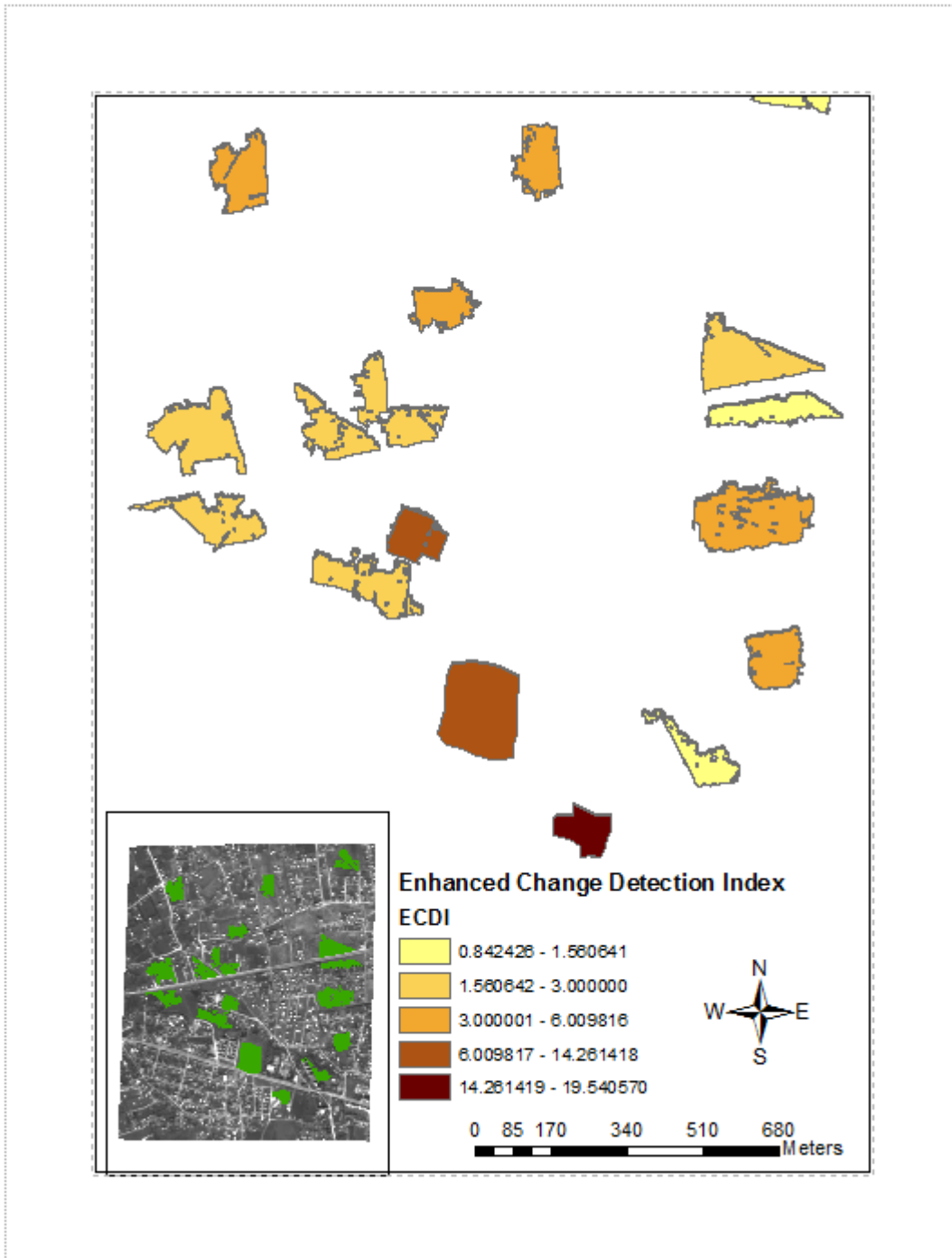


Figure 3.28 The Enhanced Change Detection Index obtained for each of the open spaces.

## 4 Conclusions and Future Work

Many issues surround post-disaster recovery and reconstruction, usually requiring a combined effort of planners, government authorities and community interaction. However, natural disasters produce an unusual set of constraints and tensions which make each case of recovery individually difficult, requiring precise consideration of the existing area. In turn, attempts need to be made with respect to re-housing but also ensuring the restoration of economy and infrastructure.

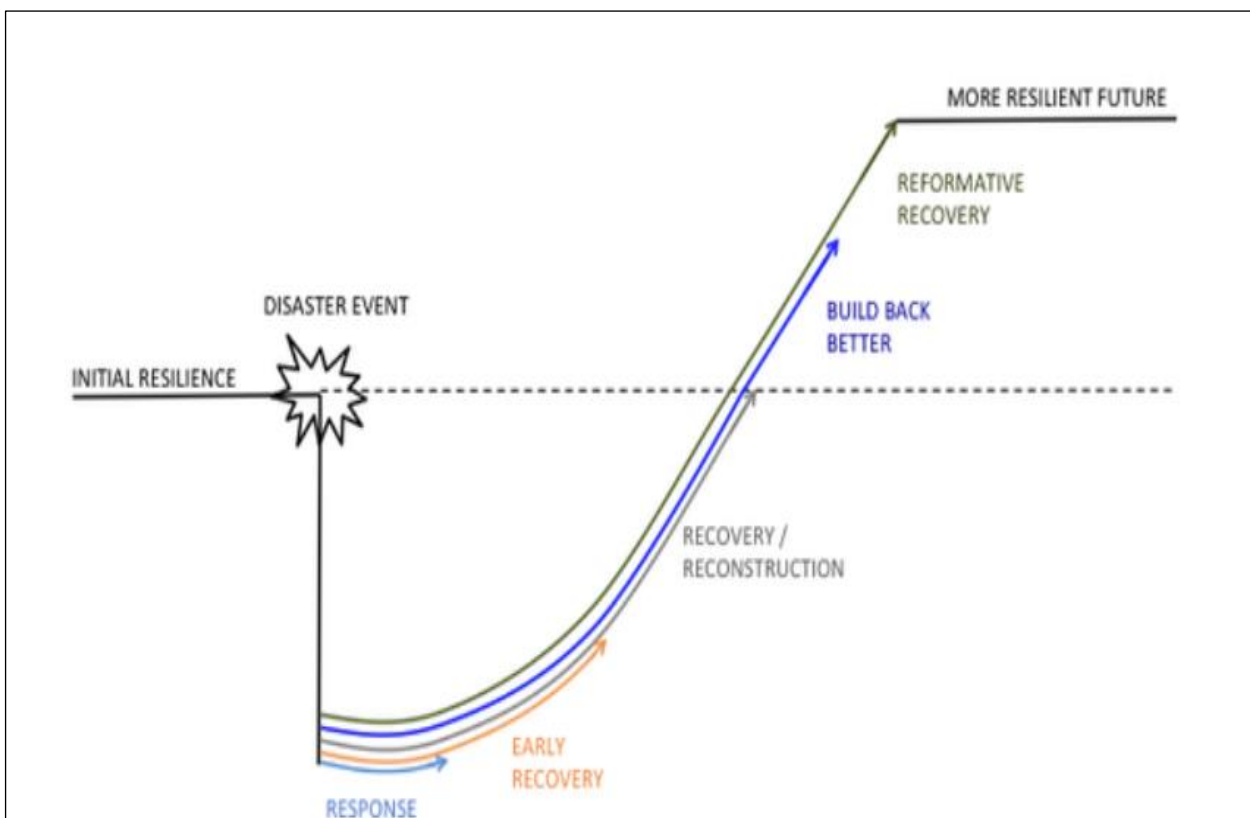


Figure 4.1 Idealised recovery curve (Lallement, 2013)

The idea after a disaster is to build back better, to create a more resilient future for a community that was adversely affected by a natural disaster event. It was therefore the ambition of SENSUM WP5 to provide the right tools to assist this process.

## REFERENCES

Brown, D. (2013) Geospatial Tools to Support Post-Disaster Recovery. *ReBuiIDD Workshop: Geospatial tools and information needs in post-disaster recovery*. Cambridge, UK. 29th March 2012.

Giada, S., T. De Groeve, D.Ehrlich, and P. Soille. 2003. Information extraction from very high resolution satellite imagery over Lukole refugee camp, Tanzania. *International Journal of Remote Sensing* 24, (22)(November): 4251-4266.

Bjorgo, E.,2000b,Using very high spatial resolution multispectral satellite sensor imagery to monitor refugee camps, *International Journal of Remote Sensing*, vol. 21, pp. 611 -616.

Lallement, D. (2013) Building post-disaster resilience into reconstruction via resilient urbanism. Collaborative Blog. [http// resilienturbanism.org/author/dlallement/](http://resilienturbanism.org/author/dlallement/) (assessed 10 June 2014)

### **Website references**

#### **1. DLR**

*Damage Assessment Maps and Geographic Reference Maps*

[Available at <http://zki.dlr.de/articale/2135p>]